

FLAVOURDYNAMICS*

A. PICH

*Departament de Física Teòrica and IFIC, Universitat de València – CSIC,
 Dr. Moliner 50, E-46100 Burjassot, València, Spain*

ABSTRACT

These lectures provide an introductory overview of the dynamics of flavour-changing transitions. The main emphasis is put on present tests of the quark-mixing matrix structure and the phenomenological determination of its parameters. The interplay of strong interactions in weak decays and the important role of flavour symmetries for controlling the size of QCD corrections to some semileptonic transitions are discussed.

1. Flavour Structure of the Standard Model

The Standard Model (SM) is a gauge theory, based on the group $SU(3)_C \otimes SU(2)_L \otimes U(1)_Y$, which describes strong, weak and electromagnetic interactions, via the exchange of the corresponding spin-1 gauge fields: 8 massless gluons and 1 massless photon for the strong and electromagnetic interactions, respectively, and 3 massive bosons, W^\pm and Z , for the weak interaction. The fermionic matter content is given by the known leptons and quarks, which are organized in a 3-fold family structure:

$$\begin{bmatrix} \nu_e & u \\ e^- & d \end{bmatrix}, \quad \begin{bmatrix} \nu_\mu & c \\ \mu^- & s \end{bmatrix}, \quad \begin{bmatrix} \nu_\tau & t \\ \tau^- & b \end{bmatrix}, \quad (1.1)$$

where (each quark appears in 3 different *colours*)

$$\begin{bmatrix} \nu_l & q_u \\ l^- & q_d \end{bmatrix} \equiv \begin{pmatrix} \nu_l \\ l^- \end{pmatrix}_L, \quad \begin{pmatrix} q_u \\ q_d \end{pmatrix}_L, \quad l^-_R, \quad (q_u)_R, \quad (q_d)_R, \quad (1.2)$$

plus the corresponding antiparticles. Thus, the left-handed fields are $SU(2)_L$ doublets, while their right-handed partners transform as $SU(2)_L$ singlets. The 3 fermionic families in (1.1) appear to have identical properties (gauge interactions); they only differ by their mass and their flavour quantum number.

The gauge symmetry is broken by the vacuum, which triggers the Spontaneous Symmetry Breaking (SSB) of the electroweak group to the electromagnetic subgroup:

$$SU(3)_C \otimes SU(2)_L \otimes U(1)_Y \xrightarrow{\text{SSB}} SU(3)_C \otimes U(1)_{QED}. \quad (1.3)$$

*Lectures given at the XXIII International Meeting on Fundamental Physics, Comillas (Spain) 22–26 May 1995

The SSB mechanism generates the masses of the weak gauge bosons, and gives rise to the appearance of a physical scalar particle in the model, the so-called *Higgs*. The fermion masses and mixings are also generated through the SSB mechanism.

The SM constitutes one of the most successful achievements in modern physics. It provides a very elegant theoretical framework, which is able to describe all known experimental facts in particle physics. A detailed description of the SM and its present phenomenological status can be found in Refs. 1 and 2, which discuss the electroweak and strong sectors, respectively.

In spite of its enormous phenomenological success, the SM leaves too many unanswered questions to be considered as a complete description of the fundamental forces. We do not understand yet why fermions are replicated in three (and only three) nearly identical copies? Why the pattern of masses and mixings is what it is? Are the masses the only difference among the three families? What is the origin of the SM flavour structure? Which dynamics is responsible for the observed CP violation?

The fermionic flavour is the main source of arbitrary free parameters in the SM: 9 fermion masses, 3 mixing angles and 1 complex phase (assuming the neutrinos to be massless). The problem of fermion–mass generation is deeply related with the mechanism responsible for the SSB. Thus, the origin of these parameters lies in the most obscure part of the SM Lagrangian: the scalar sector. Clearly, the dynamics of flavour appears to be “terra incognita” which deserves a careful investigation.

The flavour structure looks richer in the quark sector, where mixing phenomena among the different families occurs (leptons would also mix if neutrino masses were non-vanishing). A precise measurement of the quark mixings would allow to test their predicted unitarity structure, and could give some hints about the unknown underlying dynamics. Since quarks are confined within hadrons, an accurate determination of their mixing parameters requires first a good understanding of hadronization effects in flavour–changing transitions. The interplay of strong interactions in weak decays plays a crucial role, which, unfortunately, is rather difficult to control due to the non-perturbative character of QCD at long distances.

The purpose of these lectures is to provide an introductory overview of our present knowledge on the quark–mixing couplings and the prospects for further improvements. I will try to emphasize those theoretical aspects which are more relevant for our understanding of the flavour–changing dynamics. Further experimental considerations are discussed elsewhere in these proceedings.

1.1. Charged–Current Interactions

In the SM flavour–changing transitions occur only in the charged–current sector:

$$\mathcal{L}_{CC} = \frac{g}{2\sqrt{2}} \left\{ W_\mu^\dagger \left[\sum_{ij} \bar{u}_i \gamma^\mu (1 - \gamma_5) \mathbf{V}_{ij} d_j + \sum_l \bar{\nu}_l \gamma^\mu (1 - \gamma_5) l \right] + \text{h.c.} \right\}. \quad (1.4)$$

The so-called Cabibbo³–Kobayashi–Maskawa⁴ (CKM) matrix \mathbf{V} couples any *up-type* quark with all *down-type* quarks. It originates from the same Yukawa couplings giving rise to the quark masses.

Before SSB, there is no mixing among the different quarks. In order to understand the origin of the matrix \mathbf{V} , let us consider the general case of N_G generations of fermions, and denote ν'_j, l'_j, u'_j, d'_j the members of the weak family j ($j = 1, \dots, N_G$), with definite transformation properties under the gauge group. The W boson couples to these fields as in Eq. (1.4), but without any mixing matrix \mathbf{V} (i.e., with $\mathbf{V}_{ij} = \delta_{ij}$).

The SSB mechanism generates fermion masses proportional to the vacuum expectation value of the scalar field, $\langle \emptyset | \phi^{(0)} | \emptyset \rangle \equiv v/\sqrt{2}$. The resulting quark–mass eigenstates are however not the same as the eigenstates of the weak interactions. The most general Yukawa Lagrangian,

$$\begin{aligned} \mathcal{L}_Y = \sum_{jk} \left\{ (\bar{u}'_j, \bar{d}'_j)_L \left[c_{jk}^{(d)} \begin{pmatrix} \phi^{(+)} \\ \phi^{(0)} \end{pmatrix} d'_{kR} + c_{jk}^{(u)} \begin{pmatrix} \phi^{(0)\dagger} \\ -\phi^{(+)\dagger} \end{pmatrix} u'_{kR} \right] \right. \\ \left. + (\bar{\nu}'_j, \bar{l}'_j)_L c_{jk}^{(l)} \begin{pmatrix} \phi^{(+)} \\ \phi^{(0)} \end{pmatrix} l'_{kR} \right\} + \text{h.c.}, \end{aligned} \quad (1.5)$$

is not diagonal in quark flavour, since this condition is not required by gauge invariance. Thus, the couplings $c_{jk}^{(d)}$, $c_{jk}^{(u)}$ and $c_{jk}^{(l)}$ are arbitrary constants.

After SSB, the Yukawa Lagrangian can be written as

$$\mathcal{L}_Y = - \left(1 + \frac{H}{v} \right) \{ \bar{\mathbf{d}}'_L \mathbf{M}'_d \mathbf{d}'_R + \bar{\mathbf{u}}'_L \mathbf{M}'_u \mathbf{u}'_R + \bar{\mathbf{l}}'_L \mathbf{M}'_l \mathbf{l}'_R + \text{h.c.} \}. \quad (1.6)$$

Here, \mathbf{d}' , \mathbf{u}' and \mathbf{l}' denote vectors in flavour space, and the corresponding mass matrices are given by

$$(\mathbf{M}'_d)_{ij} \equiv -c_{ij}^{(d)} v/\sqrt{2}, \quad (\mathbf{M}'_u)_{ij} \equiv -c_{ij}^{(u)} v/\sqrt{2}, \quad (\mathbf{M}'_l)_{ij} \equiv -c_{ij}^{(l)} v/\sqrt{2}. \quad (1.7)$$

The diagonalization of these matrices determines the mass eigenstates d_j , u_j and l_j .

The matrix \mathbf{M}'_d can be decomposed as $\mathbf{M}'_d = \mathbf{H}_d \mathbf{U}_d = \mathbf{S}_d^\dagger \mathbf{M}_d \mathbf{S}_d \mathbf{U}_d$, where $\mathbf{H}_d \equiv \sqrt{\mathbf{M}'_d \mathbf{M}'_d{}^\dagger}$ is an hermitian positive–definite matrix, while \mathbf{U}_d is unitary. \mathbf{H}_d can be diagonalized by a unitary matrix \mathbf{S}_d ; the resulting matrix \mathbf{M}_d is diagonal, hermitian and positive definite. Similarly, one has $\mathbf{M}'_u = \mathbf{H}_u \mathbf{U}_u = \mathbf{S}_u^\dagger \mathbf{M}_u \mathbf{S}_u \mathbf{U}_u$ and $\mathbf{M}'_l = \mathbf{H}_l \mathbf{U}_l = \mathbf{S}_l^\dagger \mathbf{M}_l \mathbf{S}_l \mathbf{U}_l$. In terms of the diagonal mass matrices, $\mathbf{M}_d = \text{diag}(m_d, m_s, m_b, \dots)$, $\mathbf{M}_u = \text{diag}(m_u, m_c, m_t, \dots)$, $\mathbf{M}_l = \text{diag}(m_e, m_\mu, m_\tau, \dots)$, the Yukawa Lagrangian takes the simpler form

$$\mathcal{L}_Y = - \left(1 + \frac{H}{v} \right) \{ \bar{\mathbf{d}} \mathbf{M}_d \mathbf{d} + \bar{\mathbf{u}} \mathbf{M}_u \mathbf{u} + \bar{\mathbf{l}} \mathbf{M}_l \mathbf{l} \}, \quad (1.8)$$

where the mass eigenstates are defined by

$$\begin{aligned} \mathbf{d}_L &\equiv \mathbf{S}_d \mathbf{d}'_L, & \mathbf{u}_L &\equiv \mathbf{S}_u \mathbf{u}'_L, & \mathbf{l}_L &\equiv \mathbf{S}_l \mathbf{l}'_L, \\ \mathbf{d}_R &\equiv \mathbf{S}_d \mathbf{U}_d \mathbf{d}'_R, & \mathbf{u}_R &\equiv \mathbf{S}_u \mathbf{U}_u \mathbf{u}'_R, & \mathbf{l}_R &\equiv \mathbf{S}_l \mathbf{U}_l \mathbf{l}'_R. \end{aligned} \quad (1.9)$$

Since, $\overline{\mathbf{f}}'_L \mathbf{f}'_L = \overline{\mathbf{f}}_L \mathbf{f}_L$ and $\overline{\mathbf{f}}'_R \mathbf{f}'_R = \overline{\mathbf{f}}_R \mathbf{f}_R$ ($f = d, u, l$), the form of the neutral-current part of the $SU(2)_L \otimes U(1)_Y$ Lagrangian does not change when expressed in terms of mass eigenstates. Therefore, there are no flavour-changing neutral currents in the SM (GIM mechanism⁵). This is a consequence of treating all equal-charge fermions on the same footing. However, $\overline{\mathbf{u}}'_L \mathbf{d}'_L = \overline{\mathbf{u}}_L \mathbf{S}_u \mathbf{S}_d^\dagger \mathbf{d}_L \equiv \overline{\mathbf{u}}_L \mathbf{V} \mathbf{d}_L$. In general, $\mathbf{S}_u \neq \mathbf{S}_d$; thus a $N_G \times N_G$ unitary mixing matrix \mathbf{V} appears in the quark charged-current sector, and one gets the Lagrangian in Eq. (1.4).

We can redefine the neutrino flavours in such a way as to eliminate the analogous mixing in the lepton sector: $\overline{\nu}'_L \mathbf{l}'_L = \overline{\nu}_L \mathbf{S}_l^\dagger \mathbf{l}_L \equiv \overline{\nu}_L \mathbf{l}_L$. The lepton flavour is then conserved in the minimal SM without right-handed neutrinos.

The fermion masses and the quark-mixing matrix \mathbf{V} are all determined by the Yukawa couplings in Eq. (1.5). However, the Yukawas are not known; therefore we have a bunch of arbitrary parameters. A general $N_G \times N_G$ unitary matrix contains N_G^2 real parameters [$N_G(N_G - 1)/2$ moduli and $N_G(N_G + 1)/2$ phases]. In the case of \mathbf{V} , many of these parameters are irrelevant, because we can always choose arbitrary quark phases. Under the phase redefinitions $u_i \rightarrow e^{i\phi_i} u_i$ and $d_j \rightarrow e^{i\theta_j} d_j$, the mixing matrix changes as $\mathbf{V}_{ij} \rightarrow \mathbf{V}_{ij} e^{i(\theta_j - \phi_i)}$; thus, $2N_G - 1$ phases are unobservable. The number of physical free parameters in the quark-mixing matrix gets then reduced to $(N_G - 1)^2$: $N_G(N_G - 1)/2$ moduli and $(N_G - 1)(N_G - 2)/2$ phases.

In the simpler case of two generations, \mathbf{V} is determined by a single parameter, the so-called Cabibbo angle³:

$$\mathbf{V} = \begin{bmatrix} \cos \theta_C & \sin \theta_C \\ -\sin \theta_C & \cos \theta_C \end{bmatrix}. \quad (1.10)$$

With $N_G = 3$, the CKM matrix is described by 3 angles and 1 phase.⁴ Different (but equivalent) representations can be found in the literature. The Particle Data Group⁶ advocates the use of the following one as the *standard* CKM parametrization:

$$\mathbf{V} = \begin{bmatrix} c_{12}c_{13} & s_{12}c_{13} & s_{13}e^{-i\delta_{13}} \\ -s_{12}c_{23} - c_{12}s_{23}s_{13}e^{i\delta_{13}} & c_{12}c_{23} - s_{12}s_{23}s_{13}e^{i\delta_{13}} & s_{23}c_{13} \\ s_{12}s_{23} - c_{12}c_{23}s_{13}e^{i\delta_{13}} & -c_{12}s_{23} - s_{12}c_{23}s_{13}e^{i\delta_{13}} & c_{23}c_{13} \end{bmatrix}. \quad (1.11)$$

Here $c_{ij} \equiv \cos \theta_{ij}$ and $s_{ij} \equiv \sin \theta_{ij}$, with i and j being generation labels ($i, j = 1, 2, 3$). The real angles θ_{12} , θ_{23} and θ_{13} can all be made to lie in the first quadrant, by an appropriate redefinition of quark field phases; then, $c_{ij} \geq 0$, $s_{ij} \geq 0$ and $0 \leq \delta_{13} \leq 2\pi$.

δ_{13} is the only complex phase in the SM Lagrangian; thus, it is a unique source of CP-violation. In fact, it was for this reason that the third generation was assumed to exist,⁴ before the discovery of the τ and the b . With two generations, the SM could not explain the observed CP-violation in the K system.

1.2. Fermion Mass Spectrum

The measured lepton masses,^{6,7}

$$\begin{aligned} m_e &= (0.51099906 \pm 0.00000015) \text{ MeV}, \\ m_\mu &= (105.658389 \pm 0.000034) \text{ MeV}, \\ m_\tau &= (1777.0 \pm 0.3) \text{ MeV}, \end{aligned} \tag{1.12}$$

are very different. This indicates a hierarchy of the original Yukawa couplings, which increase from one generation to the other. A similar pattern is found in the quark spectrum:^{8,9,10,11,12,13,14,15,16,17,18}

$$\begin{aligned} \overline{m}_d(1 \text{ GeV}) &= (8.5 \pm 2.5) \text{ MeV}, & \overline{m}_u(1 \text{ GeV}) &= (5.0 \pm 2.5) \text{ MeV}, \\ \overline{m}_s(1 \text{ GeV}) &= (180 \pm 25) \text{ MeV}, & \overline{m}_c &= (1.25 \pm 0.05) \text{ GeV}, \\ \overline{m}_b &= (4.25 \pm 0.10) \text{ GeV}, & m_t &= (180 \pm 12) \text{ GeV}. \end{aligned} \tag{1.13}$$

Since $m_d > m_u$, the first quark family behaves analogously to the lepton ones, where the heavier states (the charged leptons) correspond to the $T_3 = -1/2$ members of the weak doublets. However, the second and third quark generations show the opposite behaviour: the up-type quarks are heavier than their doublet partners.

The present experimental bounds^{6,19} on the neutrino masses are:

$$m_{\nu_e} < 7.0 \text{ eV (95\% CL)}, \quad m_{\nu_\mu} < 0.27 \text{ MeV (90\% CL)}, \quad m_{\nu_\tau} < 24 \text{ MeV (95\% CL)}. \tag{1.14}$$

At this point, one should make a word of caution concerning quark masses. Since quarks are confined within hadrons, the kinematical concept of (*on-shell*) quark mass, corresponding to a free asymptotic state, is meaningless. What we call quark masses are the parameters appearing in the mass term of the QCD Lagrangian (the so-called *current* quark masses). Like any other coupling, these parameters need to be appropriately defined within some renormalization scheme. Thus, they depend on the chosen renormalization scheme (we use the \overline{MS} scheme) and are functions of the renormalization scale; i.e., masses are *running* parameters which we denote by $\overline{m}(\mu)$.

One can adopt the value of the running mass at the scale $\mu = m_q$ to characterize the quark mass, i.e. $\overline{m}_q \equiv \overline{m}_q(\overline{m}_q)$. This is not possible for the light flavours because our perturbative QCD formulae are no longer valid at such low scales; this is why the up, down and strange quark masses in (1.13) have been normalized at a common reference scale $\mu = 1 \text{ GeV}$. The phenomenological determination of these masses suffers from rather large uncertainties.

Using the chiral symmetry properties of the light-quark sector,^{20,21} one can fix more precisely the ratios^{8,9,20}

$$\frac{2m_s}{m_d + m_u} = 22.6 \pm 3.3, \quad \frac{m_d - m_u}{m_d + m_u} = 0.25 \pm 0.04, \tag{1.15}$$

which do not have any scale or scheme dependence (QCD is flavour blind).

For heavy quarks, one can also define the mass as the pole of the quark propagator. This quantity would correspond to the kinematical *on-shell* mass measured in the leptonic case. The only problem is that there should not be any pole for confined quarks. Nevertheless, the definition of *pole* mass still makes sense within perturbation theory. The relation between the perturbative *pole* mass and the *running* mass is:^{22,23}

$$m_q^{\text{pole}} = \overline{m}_q(m_q^{\text{pole}}) \left\{ 1 + \frac{4}{3} \frac{\alpha_s(m_q^{\text{pole}})}{\pi} + O(\alpha_s^2) \right\}. \quad (1.16)$$

The numerical difference between these two definitions is quite important. Even at the top-mass scale where α_s is small one has $m_t^{\text{pole}} - \overline{m}_t \sim 7$ GeV, which is of the same size as the present experimental uncertainty. Thus, when quoting any numerical values for quark masses, it is very important to specify the exact definition to which they refer. The measured value of m_t given in (1.13) seems to correspond to a *pole* mass (we will assume that in the following); however, the adopted definition has not been given in the published experimental papers.^{17,18}

2. Weak Decays

2.1. $\mu^- \rightarrow e^- \bar{\nu}_e \nu_\mu$

The simplest flavour-changing process is the leptonic decay of the muon, which proceeds through the W -exchange diagram shown in Fig. 1. The momentum transfer carried by the intermediate W is very small compared to M_W . Therefore, the vector-boson propagator reduces to a contact interaction,

$$\frac{-g_{\mu\nu} + q_\mu q_\nu / M_W^2}{q^2 - M_W^2} \xrightarrow{q^2 \ll M_W^2} \frac{g_{\mu\nu}}{M_W^2}. \quad (2.1)$$

The decay can then be described through an effective local 4-fermion Hamiltonian,

$$\mathcal{H}_{\text{eff}} = \frac{G_F}{\sqrt{2}} [\bar{e} \gamma^\alpha (1 - \gamma_5) \nu_e] [\bar{\nu}_\mu \gamma_\alpha (1 - \gamma_5) \mu], \quad (2.2)$$

where

$$\frac{G_F}{\sqrt{2}} = \frac{g^2}{8M_W^2} \quad (2.3)$$

is called the Fermi coupling constant. G_F is fixed by the total decay width,

$$\frac{1}{\tau_\mu} = \Gamma(\mu^- \rightarrow e^- \bar{\nu}_e \nu_\mu) = \frac{G_F^2 m_\mu^5}{192\pi^3} (1 + \delta_{\text{RC}}) f(m_e^2/m_\mu^2), \quad (2.4)$$

where $f(x) = 1 - 8x + 8x^3 - x^4 - 12x^2 \ln x$, and

$$(1 + \delta_{\text{RC}}) = \left[1 + \frac{\alpha}{2\pi} \left(\frac{25}{4} - \pi^2 \right) \right] \left[1 + \frac{3}{5} \frac{m_\mu^2}{M_W^2} - 2 \frac{m_e^2}{M_W^2} \right] = 0.9958 \quad (2.5)$$

takes into account the leading higher-order corrections.²⁴ The measured lifetime,⁶ $\tau_\mu = (2.19703 \pm 0.00004) \times 10^{-6}$ s, implies the value

$$G_F = (1.16639 \pm 0.00002) \times 10^{-5} \text{ GeV}^{-2} \approx \frac{1}{(293 \text{ GeV})^2}. \quad (2.6)$$

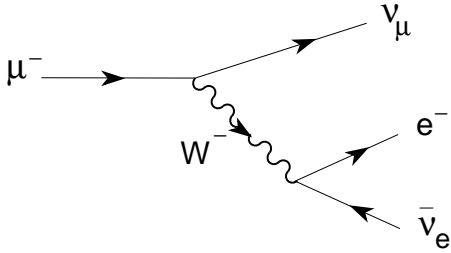


Figure 1: μ -decay diagram.

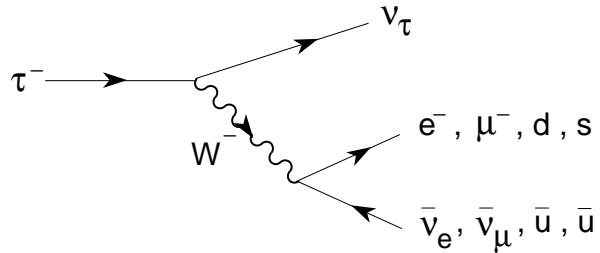


Figure 2: τ -decay diagram.

2.2. τ Decay

The decays of the τ lepton proceed through the same W -exchange mechanism as the leptonic μ decay. The only difference is that several final states are kinematically allowed: $\tau^- \rightarrow \nu_\tau e^- \bar{\nu}_e$, $\tau^- \rightarrow \nu_\tau \mu^- \bar{\nu}_\mu$, $\tau^- \rightarrow \nu_\tau d \bar{u}$ and $\tau^- \rightarrow \nu_\tau s \bar{u}$. Owing to the universality of the W -couplings, all these decay modes have equal amplitudes (if final fermion masses and QCD interactions are neglected), except for an additional $N_C |\mathbf{V}_{ui}|^2$ factor ($i = d, s$) in the semileptonic channels, where $N_C = 3$ is the number of quark colours. Making trivial kinematical changes in Eq. (2.4), one easily gets the lowest-order prediction for the total τ decay width:

$$\frac{1}{\tau_\tau} \equiv \Gamma(\tau) \approx \Gamma(\mu) \left(\frac{m_\tau}{m_\mu} \right)^5 \left\{ 2 + N_C (|\mathbf{V}_{ud}|^2 + |\mathbf{V}_{us}|^2) \right\} \approx \frac{5}{\tau_\mu} \left(\frac{m_\tau}{m_\mu} \right)^5, \quad (2.7)$$

where we have used the CKM unitarity relation $|\mathbf{V}_{ud}|^2 + |\mathbf{V}_{us}|^2 = 1 - |\mathbf{V}_{ub}|^2 \approx 1$ (we will see later that this is an excellent approximation). From the measured muon lifetime, one has then $\tau_\tau \approx 3.3 \times 10^{-13}$ s, to be compared with the experimental value²⁵ $\tau_\tau^{\text{exp}} = (2.916 \pm 0.016) \times 10^{-13}$ s.

The branching ratios into the different decay modes are predicted to be:

$$\begin{aligned} \text{Br}(\tau^- \rightarrow \nu_\tau e^- \bar{\nu}_e) &\approx \frac{1}{5} = 20\% && [\text{exp: } (17.79 \pm 0.09)\%], \\ \frac{\text{Br}(\tau^- \rightarrow \nu_\tau \mu^- \bar{\nu}_\mu)}{\text{Br}(\tau^- \rightarrow \nu_\tau e^- \bar{\nu}_e)} &\approx \frac{f(m_\mu^2/m_\tau^2)}{f(m_e^2/m_\tau^2)} = 0.97256 && [\text{exp: } 0.974 \pm 0.007], \\ R_\tau \equiv \frac{\Gamma(\tau \rightarrow \nu_\tau + \text{Hadrons})}{\Gamma(\tau^- \rightarrow \nu_\tau e^- \bar{\nu}_e)} &\approx N_C && [\text{exp: } 3.647 \pm 0.024], \end{aligned} \quad (2.8)$$

in good agreement with the measured numbers,²⁵ indicated on the right. Our naive predictions only deviate from the experimental results by about 20%. A much better agreement is obtained for the absolute value of the leptonic decay widths:

$$\Gamma(\tau^- \rightarrow \nu_\tau e^- \bar{\nu}_e) \approx \frac{1}{\tau_\mu} \left(\frac{m_\tau}{m_\mu} \right)^5 = 6.12 \times 10^{11} \text{ s}^{-1} \quad [\text{exp: } (6.10 \pm 0.05) \times 10^{11} \text{ s}^{-1}]. \quad (2.9)$$

The reason why this prediction works much better can be easily understood. The branching ratios are more sensitive to the corrections induced by strong interactions, which we are completely neglecting. These corrections are generated by gluonic exchanges between the final quarks and only affect the semileptonic decay modes. As indicated by the measured R_τ value, they amount to a 20% effect.

2.3. Charm Decays

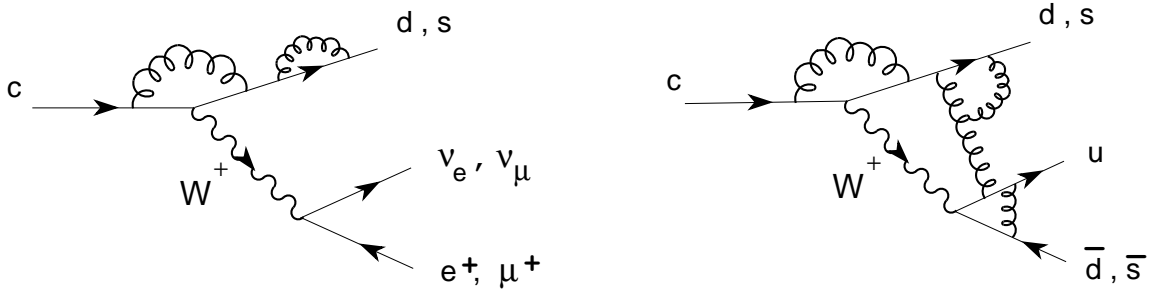


Figure 3: Feynman diagrams for semileptonic and non-leptonic c decays.

At lowest order, the decay of the charm quark is described by the same Feynman diagram as the μ and τ decays. The initial c quark converts into a d or s flavour through the emission of a W^+ ; the corresponding vertices contain a \mathbf{V}_{ci}^* ($i = d, s$) mixing factor. The emitted W^+ can give rise to several fermionic final states which are kinematically allowed: $\nu_e e^+$, $\nu_\mu \mu^+$, $u \bar{d}$ and $u \bar{s}$. Adding all possible decay modes, the total charm decay width is predicted to be

$$\Gamma(c) \approx \frac{1}{\tau_\mu} \left(\frac{m_c}{m_\mu} \right)^5 \left(|\mathbf{V}_{cd}|^2 + |\mathbf{V}_{cs}|^2 \right) \left\{ 2 + N_C \left(|\mathbf{V}_{ud}|^2 + |\mathbf{V}_{us}|^2 \right) \right\}. \quad (2.10)$$

Using the approximate relations (they would be exact with only two fermion generations) $|\mathbf{V}_{cd}|^2 + |\mathbf{V}_{cs}|^2 = 1 - |\mathbf{V}_{cb}|^2 \approx 1$ and $|\mathbf{V}_{ud}|^2 + |\mathbf{V}_{us}|^2 = 1 - |\mathbf{V}_{ub}|^2 \approx 1$, one gets a charm lifetime

$$\tau_c \approx \frac{1}{5} \tau_\mu \left(\frac{m_\mu}{m_c} \right)^5 \approx 7.6 \times 10^{-13} \text{ s}, \quad (2.11)$$

where we have taken $m_c \sim 1.5$ GeV. This estimate should be compared with the measured lifetimes of the different charm hadrons:⁶

$$\begin{aligned}\tau_{D^+} &= (10.57 \pm 0.15) \times 10^{-13} \text{ s}, & \tau_{\Lambda_c^+} &= (2.00^{+0.11}_{-0.10}) \times 10^{-13} \text{ s}, \\ \tau_{D^0} &= (4.15 \pm 0.04) \times 10^{-13} \text{ s}, & \tau_{\Xi_c^+} &= (3.5^{+0.7}_{-0.4}) \times 10^{-13} \text{ s}, \\ \tau_{D_s^+} &= (4.67 \pm 0.17) \times 10^{-13} \text{ s}, & \tau_{\Xi_c^0} &= (0.98^{+0.23}_{-0.15}) \times 10^{-13} \text{ s}.\end{aligned}\tag{2.12}$$

Obviously, changing the numerical value of m_c one could trivially fit any of those measurements. However, there is no way to understand the large splittings among the different hadronic lifetimes. Our naive estimate assumes a similar lifetime τ_c for all charm hadrons, whereas one measures⁶ $\tau(D^+)/\tau(D^0) \approx 2.5$ or $\tau(D^+)/\tau(\Xi_c^0) \approx 11$.

The prediction works substantially better for the semileptonic decay widths:

$$\Gamma(c \rightarrow X l^+ \nu_l) \equiv \frac{\text{Br}(c \rightarrow X l^+ \nu_l)}{\tau_c} \approx \frac{1}{\tau_\mu} \left(\frac{m_c}{m_\mu} \right)^5 \approx 2.6 \times 10^{11} \text{ s}^{-1},\tag{2.13}$$

to be compared with the experimental values^{6,26,27}

$$\begin{aligned}\Gamma(D^+ \rightarrow X^0 l^+ \nu_l) &= (1.63 \pm 0.18) \times 10^{11} \text{ s}^{-1}, \\ \Gamma(D^0 \rightarrow X^- l^+ \nu_l) &= (1.65 \pm 0.08) \times 10^{11} \text{ s}^{-1}, \\ \Gamma(\Lambda_c^+ \rightarrow X^0 l^+ \nu_l) &= (2.3 \pm 0.9) \times 10^{11} \text{ s}^{-1}.\end{aligned}\tag{2.14}$$

The problem with our lifetime prediction has to do with the strong interactions that we have ignored. In the semileptonic decays, gluons can only couple to a single $c \rightarrow d, s$ hadronic current; they produce then a sizeable but not too large correction. However, the hadronic decay modes contain two different quark currents and gluons can couple everywhere. The corrections induced by those gluons exchanged from one quark current to the other appear to be crucial to understand the hadronic charm decays. Notice, that QCD is more important in the semileptonic c -decay modes than in the inclusive hadronic τ -decay. This should be expected, because now we are considering decays such as $D^+ \rightarrow X^0 l^+ \nu_l$ which refer to a given charm hadron; i.e., these decays, although inclusive in the final state, are in fact exclusive with respect to the initial hadron.

2.4. Bottom Decays

Applying again the same naive arguments, one gets

$$\frac{1}{\tau_b} \equiv \Gamma(b) \approx \frac{1}{\tau_\mu} \left(\frac{m_b}{m_\mu} \right)^5 \chi^{\text{CKM}} N_{\text{eff}},\tag{2.15}$$

where

$$\begin{aligned}\chi^{\text{CKM}} &\equiv f_c |\mathbf{V}_{cb}|^2 + |\mathbf{V}_{ub}|^2, \\ N_{\text{eff}} &\equiv 2 + f_\tau + N_C \left[f'_c (|\mathbf{V}_{cd}|^2 + |\mathbf{V}_{cs}|^2) + (|\mathbf{V}_{ud}|^2 + |\mathbf{V}_{us}|^2) \right].\end{aligned}\tag{2.16}$$

Owing to the larger mass of the b , heavier final states involving charmed hadrons or the τ lepton can be now produced. Therefore, one can no longer neglect the kinematical effects induced by the non-zero final masses, which have been parametrized through the factors f_c , f_τ and f'_c . Taking $m_c \sim 1.5$ GeV and $m_b \sim 4.5$ GeV, we get the rough estimate $f_\tau \sim f_c \sim f'_c \sim f(m_c^2/m_b^2) \sim 0.5$, which implies $N_{\text{eff}} \approx 7$. We have then

$$\tau_b \approx \frac{2.2 \times 10^{-15} \text{ s}}{\chi^{\text{CKM}}} \times \left(\frac{7}{N_{\text{eff}}} \right). \quad (2.17)$$

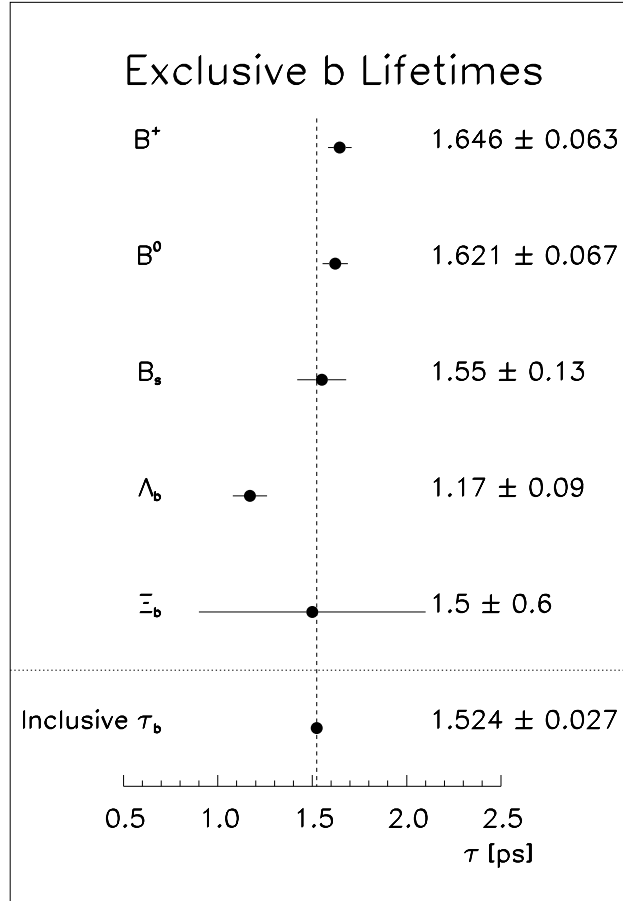


Figure 4: Measured lifetimes of the b hadrons.²⁸

The experimental lifetimes of the known b hadrons are plotted in Fig. 4. Except for τ_{Λ_b} which is slightly smaller, all hadrons turn out to have a similar lifetime. This provides some support to our approximation (2.15), which ignores hadronization effects. Using Eq. (2.17), the inclusive measurement $\tau_b = (1.524 \pm 0.027) \times 10^{-12}$ s implies $\chi^{\text{CKM}} \sim 10^{-3}$. Thus, the mixing of the bottom with the up and charm quarks is very small. The unitarity of the CKM matrix requires then $|\mathbf{V}_{tb}| \approx 1$.

Our prediction for the b semileptonic branching ratio is

$$\Gamma(b \rightarrow X l^- \bar{\nu}_l) \equiv \frac{\text{Br}(b \rightarrow X l^- \bar{\nu}_l)}{\tau_b} \approx \frac{1}{\tau_\mu} \left(\frac{m_b}{m_\mu} \right)^5 \chi^{\text{CKM}} \approx 6.4 \times 10^{13} \chi^{\text{CKM}} \text{ s}^{-1}, \quad (2.18)$$

to be compared with the experimental measurements:^{26,28}

$$\begin{aligned} \Gamma(b \rightarrow X l^- \bar{\nu}_l) &= (7.3 \pm 0.3) \times 10^{10} \text{ s}^{-1}, \\ \Gamma(\bar{B}^0 \rightarrow X^+ l^- \bar{\nu}_l) &= (6.3 \pm 0.7) \times 10^{10} \text{ s}^{-1}, \\ \Gamma(B^- \rightarrow X^0 l^- \bar{\nu}_l) &= (6.1 \pm 1.4) \times 10^{10} \text{ s}^{-1}, \\ \Gamma(B \rightarrow X \tau^- \bar{\nu}_\tau) &= (1.7 \pm 0.3) \times 10^{10} \text{ s}^{-1}. \end{aligned} \quad (2.19)$$

These numbers can be easily understood with a mixing factor $\chi^{\text{CKM}} \sim 10^{-3}$. The unknown factor χ^{CKM} cancels out in the branching ratio, which is expected to be

$$\text{Br}(b \rightarrow l^- \bar{\nu}_l X) \sim \frac{1}{N_{\text{eff}}} \sim 14\%, \quad (2.20)$$

in reasonable agreement with the measured values:^{26,28}

$$\begin{aligned} \text{Br}(b \rightarrow X l^- \bar{\nu}_l) &= (11.2 \pm 0.4)\%, \\ \text{Br}(\bar{B}^0 \rightarrow X^+ l^- \bar{\nu}_l) &= (10.2 \pm 1.0)\%, \\ \text{Br}(B^- \rightarrow X^0 l^- \bar{\nu}_l) &= (10.1 \pm 2.3)\%. \end{aligned} \quad (2.21)$$

Thus, our naive description of the quark decay process seems to work much better for the bottom than for the charm. Owing to the larger mass of the b quark, the strength of the QCD coupling is smaller, implying that the missing corrections induced by the strong interactions are not so crucial as in the charm system.

2.5. Strange Decays

Let us try to analyze the decay width of the quark s in the same way. The only kinematically allowed decays are $s \rightarrow u e^- \bar{\nu}_e$, $s \rightarrow u \mu^- \bar{\nu}_\mu$ and $s \rightarrow u d \bar{u}$. Therefore,

$$\frac{1}{\tau_s} \approx \frac{1}{\tau_\mu} \left(\frac{m_s}{m_\mu} \right)^5 |\mathbf{V}_{us}|^2 \{2 + N_C |\mathbf{V}_{ud}|^2\} \approx \frac{5 \sin^2 \theta_C}{\tau_\mu} \left(\frac{m_s}{m_\mu} \right)^5 \approx \frac{1}{4 \times 10^{-7} \text{ s}}, \quad (2.22)$$

where we have taken $|\mathbf{V}_{us}| \approx \sin \theta_C \approx 0.22$ and $m_s \approx 200$ MeV. The measured lifetimes of strange hadrons deviate strongly from this estimate:⁶

$$\begin{aligned} \tau(K_S) &= (0.8926 \pm 0.0012) \times 10^{-10} \text{ s}, & \tau(K_L) &= (5.17 \pm 0.04) \times 10^{-8} \text{ s}, \\ \tau(K^+) &= (1.2371 \pm 0.0029) \times 10^{-8} \text{ s}, & \tau(\Lambda) &= (2.632 \pm 0.020) \times 10^{-10} \text{ s}. \end{aligned} \quad (2.23)$$

This time we need to explain lifetimes which differ by two orders of magnitude: $\tau(K^+)/\tau(K_S) = 139!$

The predicted semileptonic decay width,

$$\Gamma(s \rightarrow e^- \bar{\nu}_e X) \approx \frac{1}{\tau_\mu} \left(\frac{m_s}{m_\mu} \right)^5 |\mathbf{V}_{us}|^2 \approx 5.4 \times 10^5 \text{ s}^{-1}, \quad (2.24)$$

does not agree either with the measurements:⁶

$$\begin{aligned} \Gamma(K^- \rightarrow \pi^0 e^- \bar{\nu}_e) &= (3.90 \pm 0.05) \times 10^6 \text{ s}^{-1}, \\ \Gamma(\bar{K}^0 \rightarrow \pi^+ e^- \bar{\nu}_e) &= (7.49 \pm 0.11) \times 10^6 \text{ s}^{-1}, \\ \Gamma(\Lambda \rightarrow p e^- \bar{\nu}_e) &= (3.16 \pm 0.06) \times 10^6 \text{ s}^{-1}. \end{aligned} \quad (2.25)$$

Thus, the strange decays cannot be understood with our naive description, which ignores the strong interactions. QCD is a crucial ingredient at the low scales relevant for s decays. The dramatic effect of the gluonic interactions is clearly shown by the famous enhancement of $\Delta I = 1/2$ transitions observed in K decays:⁶

$$\frac{\Gamma(K_S \rightarrow \pi^+ \pi^-)}{\Gamma(K^+ \rightarrow \pi^+ \pi^0)} = \frac{\text{Br}(K_S \rightarrow \pi^+ \pi^-) \tau(K^+)}{\text{Br}(K^+ \rightarrow \pi^+ \pi^0) \tau(K_S)} = 449. \quad (2.26)$$

This huge ratio is predicted to be four in the absence of QCD *corrections!*

3. General Analysis of Semileptonic Decays

Several important lessons can be extracted from our previous discussion of weak decays:

- Whenever hadrons (quarks) are involved, gluonic corrections play an important role in the decay amplitude.
- The interplay of QCD is stronger at lower scales. Gluonic effects are moderate in b decay, but quite sizeable (sometimes 100%) in the charm system. The strength of the strong interactions is so large at the m_s scale, that there is no way to understand the decays of strange hadrons with a free-quark description.
- The dynamical effect of the strong interaction is more important in non-leptonic transitions, where there are two different quark currents and gluons can couple everywhere. In semileptonic decays, gluons can only be exchanged within a single quark current; their contribution is then much smaller.
- Inclusive transitions are less sensitive to QCD than exclusive hadronic decays where hadronization effects are obviously crucial.

Thus, we need to worry about QCD if we want to study the quark–mixing structure of flavour–changing transitions. Unfortunately, the long–distance regime of the strong interactions is still not well understood. While the SM Lagrangian is formulated in terms of quarks and gluons, the measurable weak decays involve hadronic bound states of these fundamental constituents. Some insight into the confinement dynamics which binds quarks into hadrons is then needed, to make possible an accurate determination of the SM parameters from experimental data.

The best way to proceed is to select those processes with smaller gluonic corrections, where we have some chance to control the QCD effects. Let us consider the semileptonic weak decay $H \rightarrow H'l\bar{\nu}_l$, associated with the corresponding quark transition $d_j \rightarrow u_i l^- \bar{\nu}_l$. Since quarks are confined within hadrons, the decay amplitude

$$T[H \rightarrow H'l\bar{\nu}_l] \approx \frac{G_F}{\sqrt{2}} \mathbf{V}_{ij} \langle H' | \bar{u}_i \gamma^\mu (1 - \gamma_5) d_j | H \rangle \bar{l} \gamma_\mu (1 - \gamma_5) \nu_l \quad (3.1)$$

always involves an hadronic matrix element of the weak left current. The evaluation of this matrix element is a non-perturbative QCD problem and, therefore, introduces unavoidable theoretical uncertainties.

Usually, one looks for a semileptonic transition where the matrix element can be fixed at some kinematical point, by a symmetry principle (this will be discussed in the next section). This has the virtue of reducing the theoretical uncertainties to the level of symmetry–breaking corrections and kinematical extrapolations. The standard example is a $0^- \rightarrow 0^-$ decay such as $K \rightarrow \pi l \nu$, $D \rightarrow K l \nu$ or $B \rightarrow D l \nu$. Only the vector current can contribute in this case:

$$\langle P'(k') | \bar{u}_i \gamma^\mu d_j | P(k) \rangle = C_{PP'} \left\{ (k + k')^\mu f_+(q^2) + (k - k')^\mu f_-(q^2) \right\}. \quad (3.2)$$

Here, $C_{PP'}$ is a Clebsh–Gordan factor and $q^2 = (k - k')^2$ the momentum transfer carried by the intermediate W . The unknown strong dynamics is fully contained in the two form factors $f_\pm(q^2)$.

Since $(k - k')^\mu \bar{l} \gamma_\mu (1 - \gamma_5) \nu_l \sim m_l$, the contribution of $f_-(q^2)$ is kinematically suppressed in the e and μ modes. Moreover, since $f_-(q^2) \approx (m_{u_i} - m_{d_j})$ [see Eq. (4.11)], there is an additional strong suppression of the $f_-(q^2)$ term in the light–flavour case. The decay width can then be written as

$$\Gamma(P \rightarrow P'l\nu) \approx \frac{G_F^2 M_P^5}{192\pi^3} |\mathbf{V}_{ij}|^2 C_{PP'}^2 |f_+(0)|^2 \mathcal{I} (1 + \delta_{\text{RC}}), \quad (3.3)$$

where δ_{RC} is an electroweak radiative correction factor and \mathcal{I} denotes a phase–space integral, which in the $m_l = 0$ limit takes the form

$$\mathcal{I} \approx \int_0^{(M_P - M_{P'})^2} \frac{dq^2}{M_P^8} \lambda^{3/2}(q^2, M_P^2, M_{P'}^2) \left| \frac{f_+(q^2)}{f_+(0)} \right|^2. \quad (3.4)$$

The usual procedure to determine $|\mathbf{V}_{ij}|$ involves three steps:

1. Measure the shape of the q^2 distribution. This fixes the ratio $|f_+(q^2)/f_+(0)|$ and therefore determines \mathcal{I} .
2. Measure the total decay width Γ . Since G_F is already known from μ decay, one gets then an experimental value for the product $|f_+(0)| |\mathbf{V}_{ij}|$.
3. Get a theoretical prediction for the normalization $f_+(0)$.

The important point to realize is that theoretical input is always needed. Thus, the accuracy of the $|\mathbf{V}_{ij}|$ determination is limited by our ability to calculate the relevant hadronic input.

4. Conserved Vector Current

Symmetries are a powerful tool to derive general constraints, without entering into the detailed dynamics. Since we have not been able to solve QCD in the difficult non-perturbative regime, we would like to get at least some handle on the strong interactions through symmetry considerations.

To simplify the discussion, let us consider the electromagnetic interaction of a fermion with charge Q :

$$\mathcal{L}_{\text{QED}} = i \bar{\Psi}(x) \gamma^\mu \partial_\mu \Psi(x) - m \bar{\Psi}(x) \Psi(x) + eQ A_\mu(x) \bar{\Psi}(x) \gamma^\mu \Psi(x). \quad (4.1)$$

The strength of the QED interaction is proportional to the electric charge; i.e., $Q_u = 2/3$, $Q_d = -1/3$ and $Q_e = -1$. What is not so trivial is the fact that the hadronic charges are exactly equal to the sum of charges of their constituents quarks. For instance, the electric charge of the proton is just given by $Q_p = 2Q_u + Q_d = 1$. That protons and electrons have the same (up to a sign) charge has been experimentally verified to a very good precision:⁶

$$\left| \frac{Q_p}{Q_e} \right| - 1 < 1.0 \times 10^{-21}. \quad (4.2)$$

However, one would naively expect that the interaction of the photon with a bound hadronic state such as the proton would be quite different from the one with an elementary electron. Fig. 5 shows the effective photon couplings of the proton and the electron, once higher-order quantum corrections are taken into account. While the electron vertex only gets higher-order QED contributions, the quark constituents within the proton are affected by all kinds of gluonic exchanges. The fact that all these complicated QCD interactions finally reduce to $Q_p = -Q_e$ looks somewhat miraculous.

The quantum loop corrections generate an electromagnetic form factor; i.e., they change the tree-level coupling eQ to $eQ F_1(q^2)$, where q^2 is the squared quadrimentum of the photon. The explicit calculation shows that the tree-level coupling

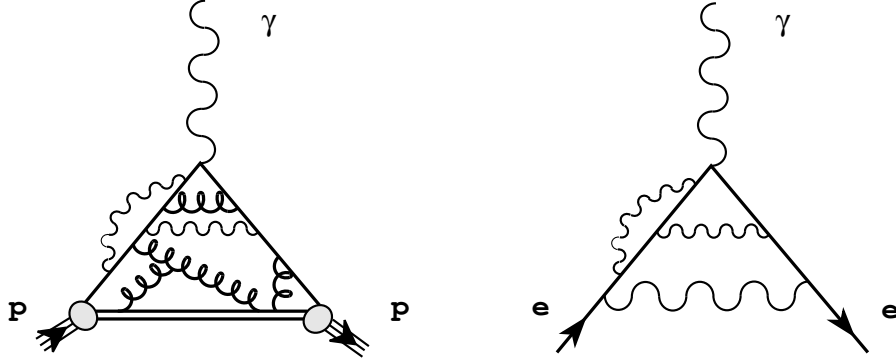


Figure 5: Electromagnetic couplings of the proton and the electron.

of an *on-shell* photon does not get modified by higher-order contributions. Although individual Feynman diagrams do generate non-zero corrections to $F_1(0)$, a complete cancellation occurs among the different contributions in such a way that the tree-level result $F_1(0) = 1$ is recovered. This is why the electric charges of the electron and the proton are finally the same (in modulus), in spite of the very different dynamics involved.

Magic cancellations of this kind usually originate from some dynamical symmetry. In QED, the symmetry at work is the invariance under phase redefinitions of the fermion fields:

$$\Psi(x) \xrightarrow{U(1)} \Psi'(x) \equiv \exp\{iQ\theta\} \Psi(x), \quad (4.3)$$

where θ is an arbitrary real constant.

A global symmetry of the Lagrangian always implies²⁹ the existence of a *conserved current*, satisfying $\partial_\mu J^\mu = 0$, and an associated *conserved charge*, $Q(t) \equiv \int d^3x J^0(\vec{x}, t)$, which is a constant of motion, i.e. $dQ(t)/dt = 0$. In the QED case, the conserved quantities are the electromagnetic vector current,

$$J_{\text{em}}^\mu = Q \bar{\Psi}(x) \gamma^\mu \Psi(x), \quad (4.4)$$

and the associated electromagnetic charge

$$Q_{\text{em}}(t) \equiv \int d^3x J_{\text{em}}^0(\vec{x}, t) = Q \int d^3x |\Psi(x)|^2 = Q. \quad (4.5)$$

It is very easy to see how the conservation of the electromagnetic current guarantees that $F_1(0) = 1$, both for the electron and the proton. In the proton case, the photon couples to the electromagnetic quark current $J_{\text{em}}^\mu = \sum_q Q_q \bar{q} \gamma^\mu q$. The proton electromagnetic vertex is then given by the hadronic matrix element

$$\begin{aligned} \langle p(k') | J_{\text{em}}^\mu(x) | p(k) \rangle &= \langle p(k') | e^{iPx} J_{\text{em}}^\mu(0) e^{-iPx} | p(k) \rangle \\ &= e^{-iqx} Q_p \bar{p}(k') \left[F_1(q^2) \gamma^\mu - iF_2(q^2) \sigma^{\mu\nu} q_\nu \right] p(k), \end{aligned} \quad (4.6)$$

where $q^\mu = (k - k')^\mu$ is the photon momentum, $p(k)$ and $\bar{p}(k')$ the Dirac spinors of the incoming and outgoing protons, and $Q_p = \sum_q Q_q$ the conserved proton charge. We have first used translation invariance to extract the x -dependence, and then a general Lorentz decomposition of the resulting amplitude, obeying the current conservation constraint $q_\mu J_{\text{em}}^\mu = 0$, has been performed. Thus, the strong dynamics is parametrized by two form factors. Taking $\mu = 0$ and integrating over d^3x , one has

$$\begin{aligned} \langle p(k') | \mathcal{Q}_{\text{em}}(t) | p(k) \rangle &= Q_p \langle p(k') | p(k) \rangle \\ &= \left[(2\pi)^3 \delta^{(3)}(q) p(k')^\dagger p(k) \right] Q_p F_1(0), \end{aligned} \quad (4.7)$$

where the first and second lines are obtained from the left- and right-hand sides of Eq. (4.6), respectively. Since $\langle p(k') | p(k) \rangle = (2\pi)^3 \delta^{(3)}(q) p(k')^\dagger p(k)$, this proves the wanted result $F_1(0) = 1$. The same derivation applies to the electron case (without the sum over constituent quarks!).

4.1. Chiral Symmetry

In the absence of quark masses, the QCD Lagrangian splits into two independent quark sectors,

$$\mathcal{L}_{\text{QCD}}^{(m=0)} = -\frac{1}{4} G_a^{\mu\nu} G_{\mu\nu}^a + i\bar{q}_L \gamma^\mu D_\mu q_L + i\bar{q}_R \gamma^\mu D_\mu q_R. \quad (4.8)$$

Here, q denotes the flavour (and colour) vector $q = \text{column}(u, d, \dots)$, and $D_\mu q$ the corresponding QCD covariant derivative. Thus, $\mathcal{L}_{\text{QCD}}^{(m=0)}$ is invariant under independent *global* $G \equiv SU(N_f)_L \otimes SU(N_f)_R$ transformations of the left- and right-handed quarks in flavour space, where N_f denotes the number of quark flavours:

$$q_L \xrightarrow{G} g_L q_L, \quad q_R \xrightarrow{G} g_R q_R, \quad g_{L,R} \in SU(N_f)_{L,R}. \quad (4.9)$$

The associated conserved currents are $L^\mu = V^\mu - A^\mu$ and $R^\mu = V^\mu + A^\mu$, with

$$V_{ij}^\mu \equiv \bar{q}_j \gamma^\mu q_i, \quad A_{ij}^\mu \equiv \bar{q}_j \gamma^\mu \gamma_5 q_i, \quad (4.10)$$

the $SU(N_f)$ multiplets of vector and axial currents. All these currents would be conserved in a massless quark world. However, the chiral symmetry is explicitly broken by the quark mass term which communicates the left- and right-handed sectors [$\mathcal{L}_{\mathcal{M}} = -(\bar{q}_R \mathcal{M} q_L + \bar{q}_L \mathcal{M}^\dagger q_R)$]. The current divergences can be easily obtained, using the QCD equations of motion:

$$\partial_\mu V_{ij}^\mu = i(m_{q_j} - m_{q_i}) \bar{q}_j q_i, \quad \partial_\mu A_{ij}^\mu = i(m_{q_j} + m_{q_i}) \bar{q}_j \gamma_5 q_i. \quad (4.11)$$

Notice, that the vector currents are still conserved for non-zero but equal quark masses [$SU(N_f)_V$ symmetry].

The light quark masses (m_u, m_d, m_s) are quite small compared with a typical hadronic scale of about 1 GeV. We have then an approximate $SU(3)_L \otimes SU(3)_R$ symmetry, leading to useful constraints.^{2,20,21} For instance, adapting the derivation given before for the electromagnetic case, it is straightforward to prove that the conservation of the vector current implies:

$$\langle p | \bar{u}\gamma^\mu d | n \rangle = \bar{p}\gamma^\mu n \quad (q^2 = 0). \quad (4.12)$$

Thus, in the isospin limit ($m_u = m_d$), strong interactions do not change the normalization of this hadronic matrix element at $q^2 = 0$.

A similar statement does not hold for the axial currents because chirality is not respected by the QCD vacuum [$\langle \emptyset | \bar{q}q | \emptyset \rangle = \langle \emptyset | (\bar{q}_L q_R + \bar{q}_R q_L) | \emptyset \rangle \neq 0$]. The chiral symmetry of the Lagrangian is spontaneously broken to its vectorial subgroup:

$$SU(3)_L \otimes SU(3)_R \xrightarrow{\text{SSB}} SU(3)_V, \quad (4.13)$$

and, according to Goldstone's theorem,³⁰ an octet of massless pseudoscalars (π, K, η) appears in the hadronic spectrum. The Goldstone nature of the pseudoscalar octet leads to many interesting implications, which go beyond the scope of these lectures (a detailed discussion can be found in Refs. 2, 20 and 21). For our present purposes, the relevant thing is that the massless pion couples to the axial current, giving rise to a pole at $q^2 = 0$ which modifies the free-quark normalization:

$$\langle p | \bar{u}\gamma^\mu \gamma_5 d | n \rangle = g_A \bar{p}\gamma^\mu n \quad (q^2 = 0), \quad (4.14)$$

where⁶ $g_A = 1.2573 \pm 0.0028 \neq 1$.

5. Determination of the CKM mixings for light quarks

The previous two sections have provided all the needed ingredients to allow an accurate determination of the CKM mixings among the up, down and strange quarks.

5.1. V_{ud}

The most accurate measurement of \mathbf{V}_{ud} is done with superallowed nuclear β decays of the Fermi type [$0^+ \rightarrow 0^+$], where the nuclear matrix element $\langle N' | \bar{u}\gamma^\mu d | N \rangle$ can be fixed by vector-current conservation. The CKM factor is obtained through the relation,³¹

$$|\mathbf{V}_{ud}|^2 = \frac{\pi^3 \ln 2}{ft G_F^2 m_e^5 (1 + \delta_{\text{RC}})} = \frac{(2984.4 \pm 0.1) \text{ s}}{ft (1 + \delta_{\text{RC}})}, \quad (5.1)$$

where the factor ft denotes a *comparative half-life* corrected for phase-space and Coulomb effects.^{32,33,34} In order to obtain $|\mathbf{V}_{ud}|$, one needs to perform a careful analysis of radiative corrections,^{35,36,37,38} including both short-distance contributions

$\Delta_{\text{inner}} = 0.0234 \pm 0.0012$, and nucleus-dependent corrections $\Delta_{\text{outer}} \equiv \delta_{\text{RC}} - \Delta_{\text{inner}}$. These radiative corrections are quite large, $\delta_{\text{RC}} \sim 3\text{--}4\%$, and have a crucial role in order to bring the results from different nuclei into good agreement. Table 1 shows the values of $|\mathbf{V}_{ud}|$ obtained from various superallowed β transitions. The final result quoted by the Particle Data Group⁶ is

$$|\mathbf{V}_{ud}| = 0.9736 \pm 0.0010. \quad (5.2)$$

Table 1: $Ft \equiv ft(1 + \Delta_{\text{outer}})$ and $|\mathbf{V}_{ud}|$ for various superallowed β decays.³¹

Nucleus	Ft	$ \mathbf{V}_{ud} $
^{14}O	3067.9 ± 2.4 s	0.9750 ± 0.0007
^{26m}Al	3071.1 ± 2.6 s	0.9744 ± 0.0007
^{34}Cl	3074.2 ± 3.1 s	0.9740 ± 0.0008
^{38m}K	3071.5 ± 3.2 s	0.9744 ± 0.0008
^{42}Sc	3077.1 ± 2.9 s	0.9735 ± 0.0008
^{46}V	3078.7 ± 3.2 s	0.9732 ± 0.0008
^{50}Mn	3073.2 ± 5.2 s	0.9741 ± 0.0010
^{54}Co	3075.1 ± 3.7 s	0.9738 ± 0.0008

An independent determination can be obtained from neutron decay, $n \rightarrow p e^- \bar{\nu}_e$. The axial current also contributes in this case; therefore, one needs to use the experimental value of the axial coupling g_A . The measured neutron lifetime,⁶ $\tau_n = 887.0 \pm 2.0$ s, implies³¹:

$$|\mathbf{V}_{ud}| = \left\{ \frac{(4904.0 \pm 5.0) \text{ s}}{\tau_n (1 + 3g_A^2)} \right\}^{1/2} = 0.981 \pm 0.002, \quad (5.3)$$

which is bigger than (5.2). Thus, a better measurement of g_A and τ_n is needed.

The pion β decay $\pi^+ \rightarrow \pi^0 e^+ \nu_e$ offers a cleaner way to measure $|\mathbf{V}_{ud}|$. It is a pure vector transition, with very small theoretical uncertainties. At $q^2 = 0$, the relevant hadronic matrix element does not receive³⁹ isospin breaking contributions of first order in $m_d - m_u$; i.e., $f_+(0) = 1 + \mathcal{O}[(m_d - m_u)^2]$. Moreover, the small available phase-space makes it possible to theoretically control the form factor with high accuracy over the entire kinematical domain. Unfortunately, owing to the kinematical suppression, this decay mode has a small branching fraction. The present experimental value is not very precise, $\text{Br}(\pi^+ \rightarrow \pi^0 e^+ \nu_e) = (1.025 \pm 0.034) \times 10^{-8}$; it implies $|\mathbf{V}_{ud}| = 0.968 \pm 0.018$. An accurate measurement of this transition would be very valuable.

5.2. V_{us}

The decays $K^+ \rightarrow \pi^0 l^+ \nu_l$ and $K^0 \rightarrow \pi^- l^+ \nu_l$ are ideal for measuring $|\mathbf{V}_{us}|$, because the relevant hadronic form factors are well understood. $SU(3)$ -breaking corrections are very suppressed and isospin violations can be easily taken into account. For $K^0 \rightarrow \pi^- l^+ \nu_l$, the $SU(3)$ symmetry relation $f_+(0) = 1$ does not get any correction linear in the quark mass differences.^{40,41} The $K^+ \rightarrow \pi^0 l^+ \nu_l$ form factor gets, however, a calculable contribution proportional to $(m_d - m_u)$, induced by π^0 - η mixing:²⁰

$$f_+^{K^0\pi^-}(0) = 1 + \mathcal{O}[(m_s - m_u)^2]; \quad f_+^{K^+\pi^0}(0) = 1 + \frac{3(m_d - m_u)}{4m_s - 2m_u - 2m_d} + \dots \quad (5.4)$$

Using Chiral Perturbation Theory methods,^{20,21} the leading higher-order corrections to (5.4) and the low-momentum behaviour of the $f_{\pm}(q^2)$ form factors can be rigorously computed. The resulting values,⁴²

$$f_+^{K^0\pi^-}(0) = 0.977, \quad f_+^{K^+\pi^0}(0)/f_+^{K^0\pi^-}(0) = 1.022, \quad (5.5)$$

should be compared with the experimental ratio⁶ $|f_+^{K^+\pi^0}(0)/f_+^{K^0\pi^-}(0)| = 1.028 \pm 0.010$. The accurate calculation of these quantities allows to extract⁴³ a precise determination of $|\mathbf{V}_{us}|$:

$$|\mathbf{V}_{us}| = 0.2196 \pm 0.0023. \quad (5.6)$$

The analysis of semileptonic hyperon decay data can also provide information on $|\mathbf{V}_{us}|$. However, the theoretical uncertainties are larger, owing to the first-order $SU(3)$ -breaking effects in the axial-vector couplings.⁴⁴ The Particle Data Group⁶ quotes the result $|\mathbf{V}_{us}| = 0.222 \pm 0.003$. The average with (5.6) gives the final value:

$$|\mathbf{V}_{us}| = 0.2205 \pm 0.0018. \quad (5.7)$$

6. \mathbf{V}_{cd} and \mathbf{V}_{cs}

$|\mathbf{V}_{cd}|$ is deduced from deep inelastic ν_{μ} and $\bar{\nu}_{\mu}$ scattering data, by measuring the dimuon production rates off valence d quarks; i.e., $\nu_{\mu}d \rightarrow \mu^- c$ with the charm quark detected through $c \rightarrow \mu^+ \nu_{\mu} d$ or $\mu^+ \nu_{\mu} s$. One gets in this way, the product⁶ $\overline{B}_c |\mathbf{V}_{cd}|^2 = (0.49 \pm 0.05) \times 10^{-2}$, where \overline{B}_c is the average semileptonic branching fraction of the produced charmed hadrons. Using⁶ $\overline{B}_c = 0.099 \pm 0.012$, yields

$$|\mathbf{V}_{cd}| = 0.224 \pm 0.016. \quad (6.1)$$

Similarly, one could extract $|\mathbf{V}_{cs}|$ from $\nu_{\mu}s \rightarrow \mu^- c$ data. The resulting values depend, however, on assumptions about the strange quark density in the parton sea. Assuming that the strange quark sea does not exceed the value corresponding to an $SU(3)$ symmetric sea, leads to the conservative lower bound⁴⁵ $|\mathbf{V}_{cs}| > 0.59$.

Better information is obtained from the decays $D \rightarrow \bar{K}l^+\nu_l$. The measured q^2 distribution⁶ can be fitted with the pole parametrization $f_+^D(q^2)/f_+^D(0) = M^2/(M^2 - q^2)$ and $M = M_{D^*} \approx 2.1$ GeV, which corresponds to the assumption that the form factor is dominated by the lightest intermediate meson with the right quantum numbers. This determines the corresponding integral \mathcal{I} , implying

$$\Gamma(D \rightarrow \bar{K}l^+\nu_l) = |f_+^D(0)|^2 |\mathbf{V}_{cs}|^2 (1.54 \times 10^{11} \text{ s}^{-1}). \quad (6.2)$$

Using²⁶ $\Gamma(D \rightarrow \bar{K}l^+\nu_l) = (8.4 \pm 0.4) \times 10^{10} \text{ s}^{-1}$, one gets then:

$$|f_+^D(0)| |\mathbf{V}_{cs}| = 0.74 \pm 0.02 \pm 0.02, \quad (6.3)$$

where the second error is from the uncertainty in the q^2 dependence.⁶

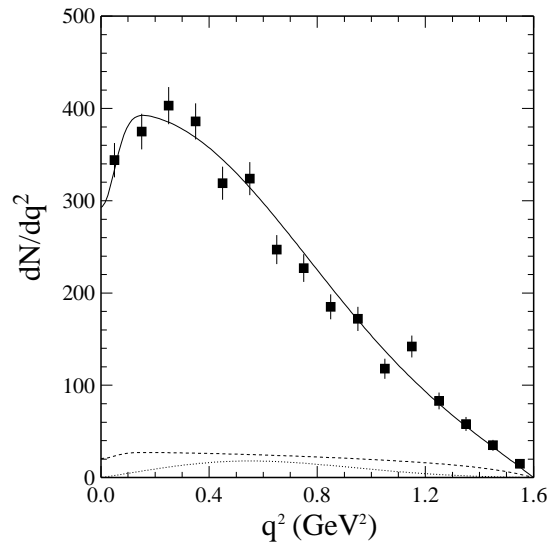


Figure 6: Measured q^2 -distribution for $D \rightarrow \bar{K}l^+\nu_l$ (CLEO II⁴⁶). The solid curve is a fit to the data with a pole form factor, which gives $M = 2.00 \pm 0.12 \pm 0.18$.

The status of our theoretical understanding of charm form factors is quite crude. The symmetry arguments are not very helpful here, because the charm-quark mass is too heavy for using the $SU(4)$ limit, and, at the same time, is too light to obtain accurate results from the opposite limit $m_c \rightarrow \infty$. Symmetry-breaking corrections are very important. The conservative assumption $|f_+^D(0)| < 1$, implies $|\mathbf{V}_{cs}| > 0.66$. Taking the range $|f_+^D(0)| = 0.75 \pm 0.15$, which covers the main part of the existing calculations, one gets:

$$|\mathbf{V}_{cs}| = 0.99 \pm 0.20. \quad (6.4)$$

Theoretical uncertainties are largely avoided by taking decay-width ratios, such as $\Gamma(D \rightarrow \pi l^+\nu_l)/\Gamma(D \rightarrow \bar{K}l^+\nu_l)$, where the form-factor uncertainty is reduced to the level of $SU(3)$ breaking. The recent CLEO II measurements⁴⁷ give

$$\left| \frac{f_+^{D\pi}(0)}{f_+^{DK}(0)} \right| \left| \frac{\mathbf{V}_{cd}}{\mathbf{V}_{cs}} \right| = 0.25 \pm 0.03. \quad (6.5)$$

Taking the conservative range $f_+^{D\pi}(0)/f_+^{DK}(0) = 1.0 \pm 0.2$, this implies

$$\left| \frac{\mathbf{V}_{cd}}{\mathbf{V}_{cs}} \right| = 0.25 \pm 0.06. \quad (6.6)$$

The present measurements of $D \rightarrow \pi l^+ \nu_l$ and $D \rightarrow \bar{K} l^+ \nu_l$ are still too poor to provide an accurate determination of the CKM factors. A 1% measurement of these semileptonic ratios seems possible⁴⁸ at a future tau–charm factory; this would allow a precise determination of $|\mathbf{V}_{cd}|/|\mathbf{V}_{cs}|$. For this to be the case, however, a better theoretical understanding of $SU(3)$ –breaking effects is mandatory. The prospects for extracting the absolute values of $|\mathbf{V}_{cd}|$ and $|\mathbf{V}_{cs}|$ with a similar accuracy are not so good; we need first to improve in a significative way our ability to control QCD effects.

7. Heavy Quark Symmetry

The chiral symmetries of massless QCD are not relevant for heavy quarks. This is the reason why we have not been able to pin down the charm CKM factors with a precision comparable to the one achieved for light quarks. There is, however, another approximate limit of QCD which turns out to be rather useful: the infinite–mass limit.

The dynamical simplifications which occur in the heavy–mass limit can be easily understood by looking back to the more familiar atomic physics. The quantum mechanical properties of an electron in the Coulomb potential of an atomic nucleus are regulated by the reduced mass $m_e M/(m_e + M) \approx m_e \ll M$, where M is the heavy nuclear mass. Therefore, different isotopes ($M \neq M'$) of the same atom ($Z = Z'$) have the same chemical properties to a very good approximation (isotopic symmetry). Moreover, atoms with nuclear spin S are $(2S + 1)$ degenerate, in the limit $M \rightarrow \infty$ (spin symmetry).

The QCD analog is slightly more complicated, but the general idea is the same. The quarks confined inside hadrons exchange momentum of a magnitude of about $\Lambda \sim M_p/3 \approx 300$ MeV. The scale Λ characterizes the typical amount by which quarks are off-shell; it also determines the hadronic size $R_{\text{had}} \sim 1/\Lambda$. If we consider a *heavy–light* hadron composed of one heavy quark Q and any number of light constituents, the light quark(s) is (are) very far off-shell by an amount of order Λ . However, if $M_Q \gg \Lambda$, the heavy quark is almost on-shell and its Compton wavelength $\lambda_Q \sim 1/M_Q$ is much smaller than the hadronic size R_{had} .

Although the quark interactions change the momentum of Q by $\delta P_Q \sim \Lambda$, its velocity only changes by a negligible amount, $\delta v_Q \sim \Lambda/M_Q \ll 1$. Thus, Q moves approximately with constant velocity. In the hadron rest frame, the heavy quark is almost at rest and acts as a static source of gluons. It is surrounded by a complicated, strongly interacting cloud of light quarks, antiquarks and gluons, sometimes referred to as the *brown muck*. To resolve the quantum numbers of the heavy quark would

require a hard probe with $Q^2 \geq M_Q^2$; however, the soft gluons coupled to the *brown muck* can only resolve larger distances of order R_{had} . The light hadronic constituents are blind to the flavour and spin orientation of the heavy quark; they only feel its colour field which extends over large distances because of confinement. Thus, in the infinite M_Q limit, the properties of heavy–light hadrons are independent of the mass (*flavour* symmetry) and spin (*spin* symmetry) of the heavy source of colour.⁴⁹

In order to put this qualitative arguments within a more formal framework, let us write the heavy quark momentum as

$$P_Q^\mu \equiv M_Q v^\mu + k^\mu, \quad (7.1)$$

where v^μ is the hadron four-velocity ($v^2 = 1$) and k^μ the *residual* momentum of order Λ . In the limit $M_Q \rightarrow \infty$ with v^μ kept fixed,⁴⁹ the QCD Feynman rules simplify considerably.⁵⁰ The heavy quark propagator becomes

$$\frac{i}{\not{P}_Q - M_Q} = \frac{i}{v \cdot k} \frac{1 + \not{v}}{2} + \mathcal{O}(k/M_Q). \quad (7.2)$$

The factors $P_\pm \equiv (1 \pm \not{v})/2$ are energy projectors ($P_\pm^2 = P_\pm$, $P_\pm P_\mp = 0$). Thus, the propagator is independent of M_Q and only the positive energy projection of the heavy quark field propagates. Moreover, since $P_+ \gamma^\mu P_+ = P_+ v^\mu P_+$, the quark–gluon vertex reduces to

$$ig \left(\frac{\lambda^a}{2} \right) \gamma^\mu \longrightarrow ig \left(\frac{\lambda^a}{2} \right) v^\mu. \quad (7.3)$$

The resulting interaction is then independent of the heavy–quark spin.

These Feynman rules can be easily incorporated into an effective Lagrangian. Making the field redefinition

$$Q(x) \approx e^{-iM_Q v \cdot x} h_v^{(Q)}(x), \quad (7.4)$$

where $h_v^{(Q)} = P_+ h_v^{(Q)} = \not{v} h_v^{(Q)}$ (i.e., we are only considering the positive–energy projection of the heavy–quark spinor), the heavy–quark Lagrangian becomes^{51,52}

$$\mathcal{L}_{\text{QCD}}^{(Q)} = \bar{Q} (i \not{D} - M_Q) Q \approx \bar{h}_v^{(Q)} i (v \cdot D) h_v^{(Q)}, \quad (7.5)$$

showing explicitly that the interaction is independent of the mass and spin of the heavy quark. The corresponding equation of motion is:

$$i \not{D} Q = M_Q Q \longrightarrow i (v \cdot D) h_v^{(Q)} = 0. \quad (7.6)$$

The phase factor in (7.4) has removed the *kinetic* piece $M_Q v^\mu$ from the heavy quark momentum, so that in momentum space a derivative acting on $h_v^{(Q)}$ just produces the *residual* momentum k^μ . Notice that $h_v^{(Q)}$ is a two–component spinor, which destroys

a quark Q but does not create the corresponding antiquark; pair creation does not occur in the heavy quark effective theory (HQET).

7.1. Spectroscopic Implications

Let us denote s_l the total spin of the light degrees of freedom in a hadron containing a single heavy quark Q . In the $M_Q \rightarrow \infty$ limit, the dynamics is independent of the heavy-quark spin. Therefore, there will be two degenerate hadronic states with $J = s_l \pm \frac{1}{2}$. For $Q\bar{q}$ mesons the ground state has negative parity and $s_l = 1/2$, giving a doublet of degenerate spin-zero and spin-one mesons. The measured charm and bottom spectrum shows indeed that this is true to a quite good approximation:⁶

$$\begin{aligned} M_{D^*} - M_D &= (142.12 \pm 0.07) \text{ MeV}, & (M_{D^*} - M_D)/M_D &\approx 8\%, \\ M_{B^*} - M_B &= (46.0 \pm 0.6) \text{ MeV}, & (M_{B^*} - M_B)/M_B &\approx 0.9\%. \end{aligned} \quad (7.7)$$

The infinite-mass limit works much better for the bottom, although the result is also good in the charm case. We expect these mass splittings to get corrections of the form $M_{P^*} - M_P \approx a/M_Q$; this gives the refined prediction $M_{B^*}^2 - M_B^2 \approx M_{D^*}^2 - M_D^2$, which is in very good agreement with the data:⁶

$$M_{D^*}^2 - M_D^2 \approx 0.53 \text{ GeV}^2, \quad M_{B^*}^2 - M_B^2 \approx 0.49 \text{ GeV}^2. \quad (7.8)$$

7.2. Weak Decay Form Factors

Let us consider the semileptonic decay $B \rightarrow Dl\bar{\nu}_l$. The decay amplitude involves the hadronic matrix element $\langle D|\bar{c}\gamma^\mu b|B\rangle$, which depends on two general form factors $f_+(q^2)$ and $f_-(q^2)$ [see Eq. (3.2)]. If the masses of the bottom and charm quarks are taken to be heavy, we can use the HQET formalism to analyze this matrix element. It is convenient to work with a mass-independent normalization for the meson states; i.e., to redefine the hadronic states as

$$|\widetilde{M}(v)\rangle \equiv \frac{1}{\sqrt{M_P}} |M(p)\rangle, \quad (7.9)$$

with the normalization $\langle \widetilde{M}(v')|\widetilde{M}(v)\rangle = 2v^0(2\pi)^3\delta^{(3)}(\vec{p} - \vec{p}')$.

In the heavy-quark theory, the wanted matrix element of the vector current takes the form⁴⁹

$$\langle \widetilde{D}(v_D)|\bar{h}_{v_D}^{(c)}\gamma^\mu h_{v_B}^{(b)}|\widetilde{B}(v_B)\rangle = \xi(v_D \cdot v_B) (v_D + v_B)^\mu, \quad (7.10)$$

where $\xi(v_D \cdot v_B)$ is an unknown form factor. That there is no term proportional to $(v_D - v_B)^\mu$ can be seen by contracting the matrix element with $(v_D - v_B)^\mu$ and using $\not{v}_B h_{v_B}^{(b)} = h_{v_B}^{(b)}$ and $\bar{h}_{v_D}^{(c)} \not{v}_D = \bar{h}_{v_D}^{(c)}$. Thus, the non-perturbative problem has

been reduced to a single form factor which only depends on the relative velocity $(v_B - v_D)^2 = 2(1 - v_B \cdot v_D)$.

The physical picture behind (7.10) is quite easy to understand. The $B \rightarrow D$ transition is induced by the action of an external vector current coupled to the heavy quark. Before the action of the current, the non-perturbative *brown muck* orbits around the heavy quark b which acts as a (static in the rest frame) colour source; the whole system moves with a velocity v_B . The effect of the current is to replace instantaneously the quark b by a quark c moving with velocity v_D . If $v_B = v_D$ nothing happens; the light quarks are unable to realize that a heavy-quark transition has taken place, because the interaction is flavour independent. However, if $v_B \neq v_D$ the *brown muck* suddenly feels itself interacting with a moving colour source. The soft-gluon exchanges needed to rearrange the light degrees of freedom into a final meson moving with velocity v_D generate a form factor suppression $\xi(v_D \cdot v_B)$, which can only depend on the Lorentz boost $\gamma = v_D \cdot v_B$ connecting the rest frames of the initial and final mesons. The flavour symmetry guarantees that this form factor is a universal function independent of the heavy mass (i.e., it is the same for $B \rightarrow B$, and $B \rightarrow D$ transitions).

When $v_B = v_D \equiv v$, the vector current $J^\mu = \bar{h}_v^{(c)} \gamma^\mu h_v^{(b)} = \bar{h}_v^{(c)} v^\mu h_v^{(b)}$ is conserved:

$$\partial_\mu J^\mu = \bar{h}_v^{(c)} (v \cdot D) h_v^{(b)} + \bar{h}_v^{(c)} (v \cdot \overleftarrow{D}) h_v^{(b)} = 0, \quad (7.11)$$

since $(v \cdot D) h_v^{(c,b)} = 0$ by the equations of motion. The associated conserved charge

$$N_{cb} \equiv \int d^3x J^0(x) = \int d^3x \bar{h}_v^{(c)\dagger} h_v^{(b)} \quad (7.12)$$

is a generator of the flavour symmetry. Acting over a B meson, it replaces a quark b by a quark c : $N_{cb} |\tilde{B}(v)\rangle = |\tilde{D}(v)\rangle$. Therefore, it satisfies

$$\langle \tilde{D}(v) | N_{cb} | \tilde{B}(v) \rangle = \langle \tilde{D}(v) | \tilde{D}(v) \rangle = 2v^0 (2\pi)^3 \delta^{(3)}(\vec{0}). \quad (7.13)$$

Comparing with Eq. (7.10) [the integration over d^3x is the same as in Eq. (4.7)], one gets the important result:

$$\xi(1) = 1. \quad (7.14)$$

This is the formal statement corresponding to the fact that the *brown muck* does not feel any change if $v_D = v_B$.

Notice, that the light- and heavy-quark symmetries allow us to pin down the normalization of the corresponding form factors at rather different kinematical points. For massless (or equal-mass) quarks, the conservation of the vector current fixes $f_+(q^2)$ at zero momentum transfer. The heavy-quark limit, however, provides information on the point of zero recoil for the D meson. Since

$$v_B \cdot v_D = \frac{M_B^2 + M_D^2 - q^2}{2M_B M_D}, \quad (7.15)$$

the equal velocity regime corresponds to the maximum momentum transfer to the final leptons: $q_{\text{max}}^2 = (M_B - M_D)^2$.

Up to now, we have only used the flavour symmetry associated with the infinite-mass limit. There is in addition a useful spin symmetry relating the $B \rightarrow D$ and $B \rightarrow D^*$ transitions. Owing to the spin-1 character of the D^* , the decay $B \rightarrow D^* l \bar{\nu}_l$ gets contributions from both the vector and the axial-vector currents. A general Lorentz parametrization would involve four independent form factors:⁵³

$$\begin{aligned} \langle D^*(p') | \bar{c} \gamma^\mu (1 - \gamma_5) b | B(p) \rangle &= \frac{2i}{M_B + M_{D^*}} \varepsilon^{\mu\nu\alpha\beta} \epsilon_\nu^* p'_\alpha p_\beta V(q^2) - 2M_{D^*} \frac{\epsilon^* \cdot q}{q^2} q^\mu A_0(q^2) \\ &- (M_B + M_{D^*}) \epsilon^{*\mu} A_1(q^2) + \frac{\epsilon^* \cdot q}{M_B + M_{D^*}} (p + p')^\mu A_2(q^2) + 2M_{D^*} \frac{\epsilon^* \cdot q}{q^2} q^\mu A_3(q^2), \end{aligned} \quad (7.16)$$

where

$$A_3(q^2) = \frac{(M_B + M_{D^*})}{2M_{D^*}} A_1(q^2) - \frac{(M_B - M_{D^*})}{2M_{D^*}} A_2(q^2); \quad A_3(0) = A_0(0). \quad (7.17)$$

In the infinite-mass limit, this matrix element reduces to the simpler expression:⁴⁹

$$\begin{aligned} \langle \widetilde{D}^*(v') | \bar{h}_{v'}^{(c)} \gamma^\mu (1 - \gamma_5) h_v^{(b)} | \widetilde{B}(v) \rangle &= i \varepsilon^{\mu\nu\alpha\beta} \epsilon_\nu^* v'_\alpha v_\beta \xi(v \cdot v') \\ &- \{ \epsilon^{*\mu} (1 + v \cdot v') - v'^\mu (\epsilon^* \cdot v) \} \xi(v \cdot v'), \end{aligned} \quad (7.18)$$

which depends on a single unknown form factor. Moreover, this form factor is precisely the same appearing in (7.10). The spin symmetry implies⁴⁹ that all $B \rightarrow D$ and $B \rightarrow D^*$ form factors are given in terms of the universal function $\xi(v \cdot v')$.

The infinite-mass limit is the starting point for a systematic expansion in powers of E/M_Q , which allows to analyze the properties of hadrons containing a heavy quark. Further details on the HQET and many other phenomenological applications can be found in Refs. 54, 55 and 56.

8. CKM mixings of the b quark

8.1. V_{cb}

The cleanest determination of $|V_{cb}|$ uses the decay $B \rightarrow D^* l \bar{\nu}_l$, where the relevant hadronic form factor can be controlled at the level of a few per cent, close to the zero-recoil region.⁵⁷ The decay $B \rightarrow D^* l \bar{\nu}_l$ has the largest branching fraction of any exclusive B decay. In addition, the relevant kinematical variable $v_B \cdot v_{D^*}$ can only vary over a small range, 1 to 1.5, where the variation of the form factors is expected to be soft and HQET techniques can be applied. Compared with the analogous decay into a pseudoscalar meson, $B \rightarrow D l \bar{\nu}_l$, the vector mode has two important advantages: 1) The $B \rightarrow D^*$ matrix element does not get any $1/M_Q$ correction⁵⁸ at

zero recoil; corrections to the infinite-mass limit are then of order $1/M_Q^2$. 2) Whereas $\Gamma(B \rightarrow D l \bar{\nu}_l)$ has a suppression factor $|\vec{p}_D|^3$ at $|\vec{p}_D| = 0$ [see Eq. (3.4)], such a suppression is not present in the $B \rightarrow D^* l \bar{\nu}_l$ decay mode.

The differential decay distribution is proportional to $|\mathbf{V}_{cb}|^2 |\mathcal{F}(v_B \cdot v_{D^*})|^2$, where the form factor $\mathcal{F}(y)$ coincides with $\xi(y)$, up to symmetry-breaking corrections of order $\alpha_s(M_Q)$ and Λ^2/M_Q^2 . The calculated short-distance QCD corrections^{59,60,61,62,63,64,65,66} and the present estimates of the $1/M_Q^2$ contributions^{67,68,69,70} result in⁷¹

$$\mathcal{F}(1) = 0.91 \pm 0.04. \quad (8.1)$$

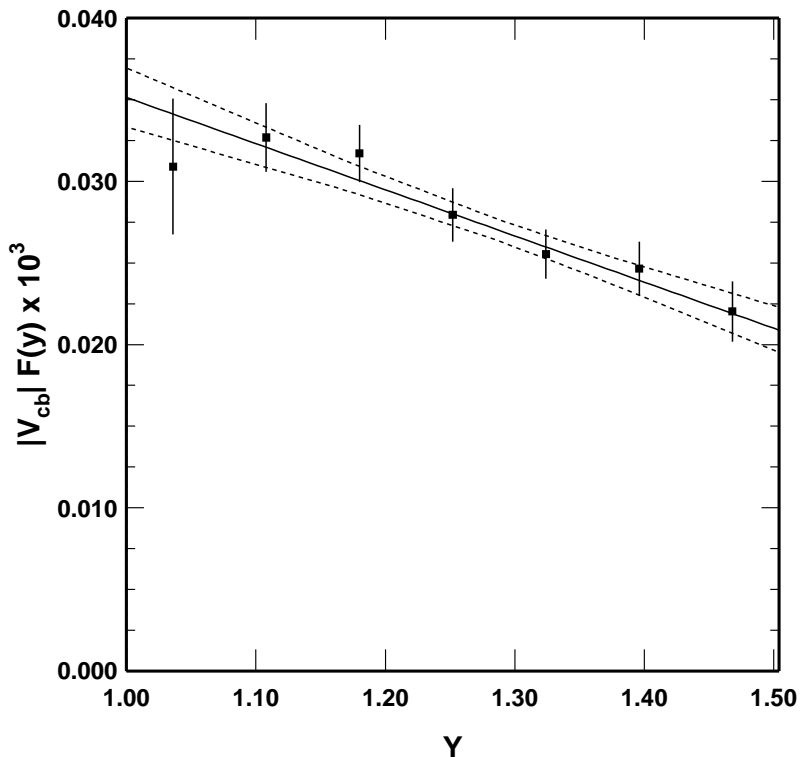


Figure 7: Measured CLEO II distribution^{28,73} of $|\mathbf{V}_{cb}| \mathcal{F}(y) \times 10^3$ ($y \equiv v_B \cdot v_{D^*}$). The curves show a linear fit to $\mathcal{F}(y)$ and the $\pm 1\sigma$ variations in the fit parameters.

The measurement of the D^* recoil spectrum has been performed by several experiments.^{72,73,74,75} Extrapolating the data to the zero-recoil point, the present world average gives⁷¹

$$|\mathbf{V}_{cb}| |\mathcal{F}(1)| = (35.1 \pm 1.7_{-0.0}^{+1.4}) \times 10^{-3}. \quad (8.2)$$

Together with (8.1), this implies⁷¹ a quite accurate determination of \mathbf{V}_{cb} :

$$|\mathbf{V}_{cb}| = (38.6_{-1.9_{\text{exp}}}^{+2.4} \pm 1.7_{\text{th}}) \times 10^{-3}. \quad (8.3)$$

Assuming that the inclusive semileptonic decay width of a bottom hadron is given by the corresponding quark decay $b \rightarrow c l^- \bar{\nu}_l$, the magnitude of $|\mathbf{V}_{cb}|$ can be also

determined from the ratio of the measured semileptonic branching ratio and lifetime. However, since $\Gamma(b \rightarrow c l^- \bar{\nu}_l) \propto m_b^5 f(m_c^2/m_b^2)$, this method is very sensitive to the not so well-known values of the bottom and charm masses. The mass dependence becomes milder if one chooses m_b and $\Delta m \equiv m_b - m_c$ as independent variables⁶⁹ (this has the advantage that Δm can be better constrained with HQET methods⁶⁷). Nevertheless, the predicted semileptonic decay width gets a large uncertainty of about 11% from this source.⁷¹ The perturbative QCD corrections, which are exactly known to $\mathcal{O}(\alpha_s)$ only, are rather sizeable.^{76,77,78} In order to properly include the effect of higher-order QCD corrections, a careful analysis of the quark-mass definition is mandatory.⁷⁹ Taking also into account the small non-perturbative contributions,^{80,81,82,83} one gets⁷¹

$$|\mathbf{V}_{cb}| = (39.8 \pm 0.9_{\text{exp}} \pm 4.0_{\text{th}}) \times 10^{-3}. \quad (8.4)$$

The quoted experimental error includes additional theoretical uncertainties. The measurement of the inclusive semileptonic branching ratio faces the difficulty of separating the contributions of direct $b \rightarrow c l^- \bar{\nu}_l$ decays from the cascade process $\bar{b} \rightarrow \bar{c} X$, $\bar{c} \rightarrow \bar{s} l^- \bar{\nu}_l$. This separation introduces a significant model dependence because one needs to assume a theoretical prediction for the shape of the primary spectrum. The amount of model dependence has been significantly reduced using events with two charged leptons from the combined process $e^+ e^- \rightarrow b \bar{b} \rightarrow (c l^- \bar{\nu}_l) (\bar{c} l^+ \nu_l)$. In the absence of mixing, the primary decays give rise to a pair of oppositely charged leptons, while a cascade process would flip the lepton charge.

The good agreement between the exclusive and inclusive determinations provides a good test of the theoretical approximations involved. Combining (8.3) and (8.4), one gets finally

$$|\mathbf{V}_{cb}| = (39 \pm 2) \times 10^{-3}. \quad (8.5)$$

8.2. V_{ub}

The present determination of $|\mathbf{V}_{ub}|$ is based on measurements of the lepton momentum spectrum in inclusive $\bar{B} \rightarrow X_q l^- \bar{\nu}_l$ decays, where X_q is any hadronic state containing a quark $q = c$ or u . The experimental signature for inclusive $b \rightarrow u$ transitions is an excess of leptons beyond the kinematic limit for the transition $b \rightarrow c l^- \bar{\nu}_l$. The yield of leptons in this small portion of the Dalitz plot must be extrapolated to the full allowed kinematic range and the resulting fraction of $b \rightarrow u$ over $b \rightarrow c$ events is then converted to the CKM ratio $|\mathbf{V}_{ub}/\mathbf{V}_{cb}|$.

This procedure is obviously very sensitive to the assumed theoretical spectrum near the kinematic limit for $\bar{B} \rightarrow D l^- \bar{\nu}_l$. Using different models to estimate the systematic theoretical uncertainties, the analyses of the experimental data^{84,85} give⁶

$$|\mathbf{V}_{ub}/\mathbf{V}_{cb}| = 0.08 \pm 0.01_{\text{exp}} \pm 0.02_{\text{th}}. \quad (8.6)$$

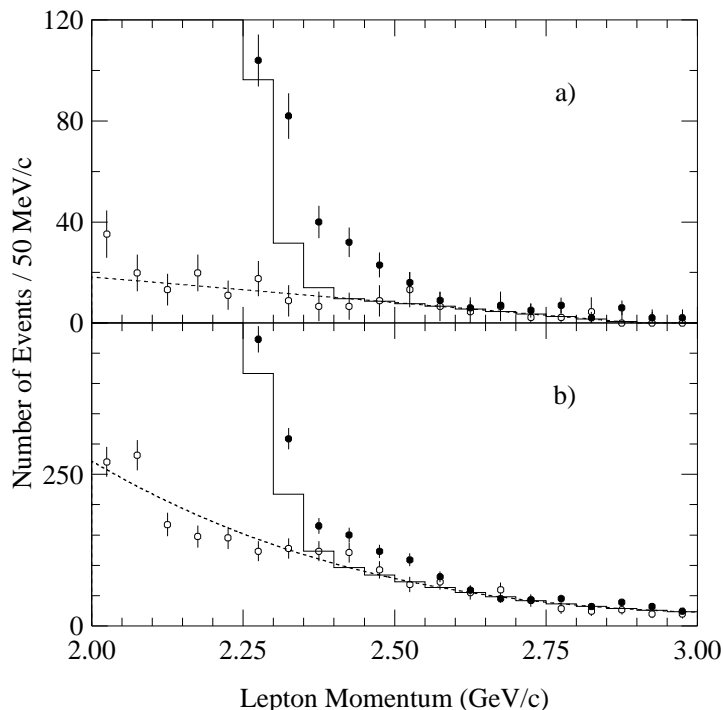


Figure 8: Inclusive lepton spectrum in the endpoint region (CLEO II⁸⁴). The two plots correspond to different experimental cuts on the same data. The filled points represent the $\Upsilon(4S)$ data, whereas data taken below the resonance are indicated by open circles and fitted with the dashed line. The solid histogram is a Monte Carlo simulation of $b \rightarrow cl\bar{\nu}_l$ processes. The excess of leptons between 2.4 and 2.6 GeV shows the existence of $b \rightarrow u$ decays.

The large model dependence of this measurement is clearly reflected by the size of the theoretical error (25%). Together with (8.5), this value implies

$$|\mathbf{V}_{ub}| = 0.003 \pm 0.001. \quad (8.7)$$

The CLEO Collaboration has recently reported⁸⁶ the first clear signal for exclusive semileptonic decays of B mesons into charmless final states:

$$\text{Br}(\bar{B} \rightarrow \pi l \bar{\nu}_l) = \begin{cases} (1.34 \pm 0.45) \times 10^{-4} & \text{(ISGW)} \\ (1.63 \pm 0.57) \times 10^{-4} & \text{(BSW)} \end{cases}; \quad (8.8)$$

$$\text{Br}(\bar{B} \rightarrow \rho l \bar{\nu}_l) = \begin{cases} (2.28^{+0.69}_{-0.83}) \times 10^{-4} & \text{(ISGW)}, \\ (3.88^{+1.15}_{-1.39}) \times 10^{-4} & \text{(BSW)}, \end{cases}$$

Again, there is a significant model dependence coming from the simulation of reconstruction efficiencies. The two quoted results correspond to the theoretical models of Refs. 87 (ISGW) and 53 (BSW).

Unfortunately, heavy–quark symmetry does not help to fix the relevant form factors in heavy–to–light ($b \rightarrow u$) transitions. To extract information on the CKM mixing factor, one has then to rely in model–dependent estimates of the hadronic matrix elements. Depending on the chosen theoretical model, the CLEO measurements imply values of $|\mathbf{V}_{ub}|$ which cover a broad range from 0.002 to 0.008.⁷¹ Although this range is in good agreement with (8.7), the large theoretical uncertainty is rather disappointing. Clearly, there is still large room for improvements here, both on the theoretical and experimental sides. While more reliable methods to predict hadronic form factors should be developed, a good sample of measured exclusive $b \rightarrow u$ decays would allow to discriminate among the different models and improve our present theoretical tools.

8.3. V_{tb}

The top quark has just been discovered recently.^{17,18} Thus, no direct measurement of $|\mathbf{V}_{tb}|$ has been performed so far. In fact, in order to identify top–quark events, the CDF and D0 experiments have assumed that the top always decays through $t \rightarrow b W^+$; i.e., $|\mathbf{V}_{tb}| = 1$. This assumption is fully justified by the smallness of the measured CKM mixings of the b with the up and charm quarks. Using the unitarity of the CKM matrix, the experimental determinations in (8.5) and (8.7) imply

$$|\mathbf{V}_{tb}| = \left\{ 1 - |\mathbf{V}_{ub}|^2 - |\mathbf{V}_{cb}|^2 \right\}^{1/2} > 0.999 \quad (95\% \text{ CL}). \quad (8.9)$$

Nevertheless, it would be nice to have a direct measurement of this CKM factor, providing a test of the unitarity structure of the SM quark mixings. CDF has recently reported⁸⁸ a preliminary value of the $t \rightarrow Wb$ branching ratio: $\text{Br}(t \rightarrow Wb) = 0.87^{+0.13}_{-0.30} {}^{+0.13}_{-0.11}$. The agreement with the theoretical expectation ($\sim 100\%$) shows indeed that $|\mathbf{V}_{tb}| \sim \mathcal{O}(1)$; however, this determination has still a rather large error.

9. Unitarity Constraints on the CKM Matrix

The present status of direct \mathbf{V}_{ij} determinations can be easily summarized:

- The light–quark mixings $|\mathbf{V}_{ud}|$ and $|\mathbf{V}_{us}|$ are rather well known (0.1% and 0.8% accuracy, respectively). Moreover, since the theory is good, improved values could be obtained with better data on semileptonic π^+ and K decays.
- $|\mathbf{V}_{cd}|$ and $|\mathbf{V}_{cs}|$ are very badly known (7% and 20% accuracy, respectively). This could be largely improved at a tau–charm factory. For this to be the case, however, a better theoretical understanding of the strong dynamics is required.
- $|\mathbf{V}_{cb}|$ and $|\mathbf{V}_{ub}|$ are also badly known (5% and 33% accuracy, respectively). However, there are good theoretical tools available. Thus, better determinations could be easily performed at a B factory.

- Nothing is known about the CKM mixings involving the top quark, except that $|\mathbf{V}_{tb}| \sim \mathcal{O}(1)$.

The entries of the first row are already accurate enough to perform a sensible test of the unitarity of the CKM matrix:

$$|\mathbf{V}_{ud}|^2 + |\mathbf{V}_{us}|^2 + |\mathbf{V}_{ub}|^2 = 0.9965 \pm 0.0021. \quad (9.1)$$

It is important to notice that radiative corrections play here a crucial role. If one uses $|\mathbf{V}_{uj}|$ values determined without radiative corrections, the result (9.1) changes to 1.0384 ± 0.0027 , giving an apparent violation of unitarity (by many σ 's).³¹

Imposing the unitarity constraint $\mathbf{V}\mathbf{V}^\dagger = \mathbf{V}^\dagger\mathbf{V} = \mathbf{1}$ (and assuming only three generations) one can get a more precise picture of the CKM matrix. The 90% confidence limits on the magnitude of the CKM matrix elements are then⁶:

$$\mathbf{V} = \begin{bmatrix} 0.9745 \text{ to } 0.9757 & 0.219 \text{ to } 0.224 & 0.002 \text{ to } 0.005 \\ 0.218 \text{ to } 0.224 & 0.9736 \text{ to } 0.9750 & 0.036 \text{ to } 0.046 \\ 0.004 \text{ to } 0.014 & 0.034 \text{ to } 0.046 & 0.9989 \text{ to } 0.9993 \end{bmatrix}, \quad (9.2)$$

which correspond to $s_{12} = 0.219$ to 0.223 , $s_{23} = 0.036$ to 0.046 , and $s_{13} = 0.002$ to 0.005 . The ranges given here are slightly different from (but consistent with) the direct determinations mentioned before.

The CKM matrix shows a hierarchical pattern, with the diagonal elements being very close to one, the ones connecting the two first generations having a size

$$\lambda \equiv |\mathbf{V}_{us}| = 0.2205 \pm 0.0018, \quad (9.3)$$

the mixing between the second and third families being of order λ^2 , and the mixing between the first and third quark flavours having a much smaller size of about λ^3 . It is then quite practical to use the approximate parametrization⁸⁹:

$$\mathbf{V} = \begin{bmatrix} 1 - \frac{\lambda^2}{2} & \lambda & A\lambda^3(\rho - i\eta) \\ -\lambda & 1 - \frac{\lambda^2}{2} & A\lambda^2 \\ A\lambda^3(1 - \rho - i\eta) & -A\lambda^2 & 1 \end{bmatrix} + O(\lambda^4), \quad (9.4)$$

where

$$A = \frac{|\mathbf{V}_{cb}|}{\lambda^2} = 0.80 \pm 0.04, \quad \sqrt{\rho^2 + \eta^2} = \left| \frac{\mathbf{V}_{ub}}{\lambda\mathbf{V}_{cb}} \right| = 0.36 \pm 0.10. \quad (9.5)$$

Notice that when $|\mathbf{V}_{ub}|$ is very small ($s_{13} \ll 1$) the standard CKM parametrization in Eq. (1.11) only contains complex phases in \mathbf{V}_{ub} and \mathbf{V}_{td} ; i.e., it follows the same phase conventions than the matrix (9.4).

10. $B^0-\bar{B}^0$ Mixing

Additional information on the CKM parameters can be obtained from flavour-changing neutral-current transitions, occurring at the 1-loop level. An important example is provided by the mixing between the B^0 meson and its antiparticle. This process occurs through the so-called box diagrams, shown in Fig. 9, where two W bosons are exchanged between a pair of quark lines.

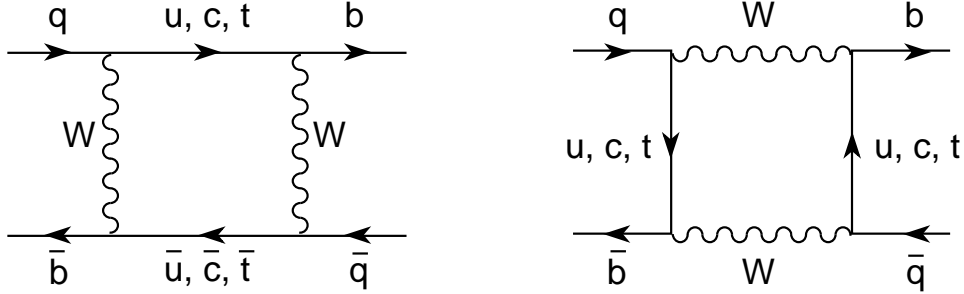


Figure 9: $B^0-\bar{B}^0$ mixing diagrams.

The mixing amplitude is proportional to

$$\langle \bar{B}_d^0 | \mathcal{H}_{\Delta B=2} | B_0 \rangle \sim \sum_{ij} \mathbf{V}_{id} \mathbf{V}_{ib}^* \mathbf{V}_{jd}^* \mathbf{V}_{jb} S(r_i, r_j), \quad (10.1)$$

where $S(r_i, r_j)$ is a loop function⁹⁰ which depends on the masses [$r_i \equiv \bar{m}_i^2/M_W^2$] of the up-type quarks running along the internal fermionic lines. Owing to the unitarity of the CKM matrix, the mixing vanishes for equal (up-type) quark masses (GIM mechanism⁵); thus the effect is proportional to the mass splittings between the u , c and t quarks. Since the different CKM factors have all a similar size, $\mathbf{V}_{ud} \mathbf{V}_{ub}^* \sim \mathbf{V}_{cd} \mathbf{V}_{cb}^* \sim \mathbf{V}_{td} \mathbf{V}_{tb}^* \sim \Lambda \lambda^3$, the final amplitude is completely dominated by the top contribution:

$$\langle \bar{B}_d^0 | \mathcal{H}_{\Delta B=2} | B_0 \rangle \sim |\mathbf{V}_{td}|^2 S(r_t, r_t). \quad (10.2)$$

This transition can then be used to perform an indirect determination of $|\mathbf{V}_{td}|$.

Notice that this determination has a qualitatively different character than the ones obtained before from tree-level weak decays. Now, we are going to test the structure of the electroweak theory at the quantum level. This flavour-changing transition could then be very sensitive to *new physics* effects occurring at higher energy scales. Moreover, the mixing amplitude crucially depends on the unitarity of the CKM matrix. Without the GIM mechanism embodied in the CKM mixing structure, the calculation of the analogous $K^0 \rightarrow \bar{K}^0$ transition (replace the b quark by a s in the box diagrams) would have failed to explain the observed $K^0-\bar{K}^0$ mixing

by several orders of magnitude.⁹¹

10.1. General Formalism for Meson–Antimeson Mixing

The flavour quantum number is not conserved by weak interactions. Thus a P^0 state ($P = K, D, B$) can be transformed into its antiparticle \bar{P}^0 . As a consequence, the flavour eigenstates P^0 and \bar{P}^0 are not mass eigenstates and do not follow an exponential decay law.

Let us consider an arbitrary mixture of the two flavour states,

$$|\psi(t)\rangle = a(t) |P^0\rangle + b(t) |\bar{P}^0\rangle \equiv \begin{pmatrix} a(t) \\ b(t) \end{pmatrix}. \quad (10.3)$$

The time evolution is governed by the equation

$$i \frac{d}{dt} |\psi(t)\rangle = \mathcal{M} |\psi(t)\rangle, \quad (10.4)$$

where \mathcal{M} is called the P^0 – \bar{P}^0 mixing matrix. Assuming CPT symmetry to hold, this 2×2 matrix can be written as

$$\mathcal{M} = \begin{pmatrix} M & M_{12} \\ M_{12}^* & M \end{pmatrix} - \frac{i}{2} \begin{pmatrix} \Gamma & \Gamma_{12} \\ \Gamma_{12}^* & \Gamma \end{pmatrix}. \quad (10.5)$$

The diagonal elements M and Γ are real parameters, which would correspond to the mass and width of the neutral mesons in the absence of mixing. The off-diagonal entries contain the *dispersive* and *absorptive* parts of the $\Delta P = 2$ transition amplitude:

$$\begin{aligned} M_{12} &= \frac{\langle P^0 | \mathcal{H}_{\Delta P=2} | \bar{P}^0 \rangle}{2M_K} + \frac{1}{2M_K} \mathcal{P} \int ds \frac{\sum_X \int dX \langle P^0 | \mathcal{H}_{\Delta P=1} | X \rangle \langle X | \mathcal{H}_{\Delta P=1} | \bar{P}^0 \rangle}{M_K^2 - s}, \\ \Gamma_{12} &= \frac{\pi}{M_K} \sum_X \int dX \delta(M_K^2 - s) \langle P^0 | \mathcal{H}_{\Delta P=1} | X \rangle \langle X | \mathcal{H}_{\Delta P=1} | \bar{P}^0 \rangle. \end{aligned} \quad (10.6)$$

The sum extends over all possible states $|X\rangle$ of invariant mass \sqrt{s} to which the $|\bar{P}^0\rangle$ can decay; the symbol dX denotes the appropriate phase-space measure, and \mathcal{P} stands for the principal value of the corresponding integral. If CP were an exact symmetry, M_{12} and Γ_{12} would also be real.

The physical eigenstates of \mathcal{M} are

$$|P_{\mp}\rangle = \frac{1}{\sqrt{|p|^2 + |q|^2}} [p |P^0\rangle \mp q |\bar{P}^0\rangle], \quad (10.7)$$

with

$$\frac{q}{p} \equiv \frac{1 - \bar{\epsilon}}{1 + \bar{\epsilon}} = \left(\frac{M_{12}^* - \frac{i}{2}\Gamma_{12}^*}{M_{12} - \frac{i}{2}\Gamma_{12}} \right)^{1/2}. \quad (10.8)$$

If M_{12} and Γ_{12} were real, then $q/p = 1$ and $|B_{\mp}\rangle$ would correspond to the CP–even and CP–odd states [we use the phase convention^a $\mathcal{CP}|P^0\rangle = -|\bar{P}^0\rangle$]

$$|P_{1,2}\rangle \equiv \frac{1}{\sqrt{2}} \left(|P^0\rangle \mp |\bar{P}^0\rangle \right), \quad \mathcal{CP} |P_{1,2}\rangle = \pm |P_{1,2}\rangle. \quad (10.9)$$

Note that if the P^0 – \bar{P}^0 mixing violates CP, the two mass eigenstates are no longer orthogonal:

$$\langle P_- | P_+ \rangle = \frac{|p|^2 - |q|^2}{|p|^2 + |q|^2} \approx 2 \operatorname{Re}(\bar{\varepsilon}). \quad (10.10)$$

The time evolution of a state which was originally produced as a P^0 or a \bar{P}^0 is given by

$$\begin{pmatrix} |P^0(t)\rangle \\ |\bar{P}^0(t)\rangle \end{pmatrix} = \begin{pmatrix} g_1(t) & \frac{q}{p}g_2(t) \\ \frac{p}{q}g_2(t) & g_1(t) \end{pmatrix} \begin{pmatrix} |P^0\rangle \\ |\bar{P}^0\rangle \end{pmatrix}, \quad (10.11)$$

where

$$\begin{pmatrix} g_1(t) \\ g_2(t) \end{pmatrix} = e^{-iMt} e^{-\Gamma t/2} \begin{pmatrix} \cos [(\Delta M - \frac{i}{2}\Delta\Gamma)t/2] \\ -i \sin [(\Delta M - \frac{i}{2}\Delta\Gamma)t/2] \end{pmatrix}, \quad (10.12)$$

with

$$\Delta M \equiv M_{P_+} - M_{P_-}, \quad \Delta\Gamma \equiv \Gamma_{P_+} - \Gamma_{P_-}. \quad (10.13)$$

The main difference between the K^0 – \bar{K}^0 and B^0 – \bar{B}^0 systems stems from the different kinematics involved. The light kaon mass only allows the hadronic decay modes $K^0 \rightarrow 2\pi$ and $K^0 \rightarrow 3\pi$. Since $\mathcal{CP}|\pi\pi\rangle = +|\pi\pi\rangle$, the CP–even kaon state decays into 2π whereas the CP–odd one decays into the phase–space suppressed 3π mode. Therefore, there is a large lifetime difference and we have a short–lived $|K_S\rangle \equiv |K_- \rangle \approx |K_1\rangle + \bar{\varepsilon}_K |K_2\rangle$ and a long–lived $|K_L\rangle \equiv |K_+ \rangle \approx |K_2\rangle + \bar{\varepsilon}_K |K_1\rangle$ kaon, with $\Gamma_{K_L} \ll \Gamma_{K_S}$. One finds experimentally that $\Delta\Gamma_{K^0} \approx -\Gamma_{K_S} \approx -2\Delta M_{K^0}$.

In the B system, there are many open decay channels and a large part of them are common to both mass eigenstates. Therefore, the $|B_{\mp}\rangle$ states have a similar lifetime; i.e., $\Delta\Gamma_{B^0} \ll \Gamma_{B^0}$. Moreover, whereas the B^0 – \bar{B}^0 transition is dominated by the top box diagram, the decay amplitudes get obviously their main contribution from the $b \rightarrow c$ transition. Thus, $\Delta\Gamma_{B^0}/\Delta M_{B^0} \sim m_b^2/m_t^2 \ll 1$.

10.2. Experimental Measurements

^a Since flavour is conserved by strong interactions, there is some freedom in defining the phases of flavour eigenstates. In general, one could use $|P_\zeta^0\rangle \equiv e^{-i\zeta}|P^0\rangle$ and $|\bar{P}_\zeta^0\rangle \equiv e^{i\zeta}|\bar{P}^0\rangle$, which satisfy $\mathcal{CP}|P_\zeta^0\rangle = -e^{-2i\zeta}|\bar{P}_\zeta^0\rangle$. Both basis are trivially related: $M_{12}^\zeta = e^{2i\zeta}M_{12}$, $\Gamma_{12}^\zeta = e^{2i\zeta}\Gamma_{12}$ and $(q/p)_\zeta = e^{-2i\zeta}(q/p)$. Thus, $q/p \neq 1$ does not necessarily imply CP violation. CP is violated in the mixing matrix if $|q/p| \neq 1$; i.e., $\operatorname{Re}(\bar{\varepsilon}) \neq 0$ and $\langle P_- | P_+ \rangle \neq 0$. Note that $\langle P_- | P_+ \rangle_\zeta = \langle P_- | P_+ \rangle$. Another phase–convention independent quantity is $(q/p)(\bar{A}_f/A_f)$, where $A_f \equiv A(P^0 \rightarrow f)$ and $\bar{A}_f \equiv A(\bar{P}^0 \rightarrow f)$, for any final state f .

With $\Delta\Gamma_{B^0}/\Delta M_{B^0} \ll 1$, the probability that a state initially produced as $|B^0\rangle$ will become $|\bar{B}^0\rangle$ at time t is given by

$$\text{Prob}[B^0 \rightarrow \bar{B}^0](t) = \frac{1}{2} e^{-\Gamma_{B^0} t} [1 - \cos(\Delta M_{B^0} t)] \equiv \frac{1}{2} e^{-\tau} [1 - \cos(x\tau)] , \quad (10.14)$$

where $\tau \equiv \Gamma_{B^0} t$ denotes the time measured in lifetime units and

$$x \equiv \frac{\Delta M_{B^0}}{\Gamma_{B^0}} \quad (10.15)$$

determines the frequency of the B^0 - \bar{B}^0 mixing oscillations. The time-integrated probability is given by

$$\chi \equiv \text{Prob}[B^0 \rightarrow \bar{B}^0] = \frac{x^2}{2(1+x^2)} . \quad (10.16)$$

Thus, $0 \leq \chi < 0.5$.

To experimentally measure the mixing transition requires the identification of the B -meson flavour at both its production and decay time. This can be done through flavour-specific decays such as $B^0 \rightarrow Xl^+\nu_l$ and $\bar{B}^0 \rightarrow Xl^-\bar{\nu}_l$. In general, mixing is measured by studying pairs of B mesons so that one B can be used to *tag* the initial flavour of the other meson. For instance, in e^+e^- machines one looks into the pair production process $e^+e^- \rightarrow B^0\bar{B}^0 \rightarrow (Xl\nu_l)(Yl\bar{\nu}_l)$. In the absence of mixing, the final leptons should have opposite charges. The amount of like-sign leptons,

$$R_{ll} \equiv \frac{N(l^\pm l^\pm)}{N(l^\pm l^\mp) + N(l^\pm l^\pm)} , \quad (10.17)$$

is then a clear signature of the mixing transition.

At high-energy colliders a B^\pm meson can be used to *tag* the flavour of the neutral B [$b\bar{b} \rightarrow B^- B^0 X \rightarrow (Yl^-\bar{\nu}_l)(Zl^\pm\nu_l)X$, $b\bar{b} \rightarrow \bar{B}^0 B^+ X \rightarrow (Yl^\mp\nu_l)(Zl^+\nu_l)X$]; then, $R_{ll} = \chi$. The relation is slightly more complicated when the *tagging* is performed through another neutral B which also oscillates. At LEP, where the two B mesons are uncorrelated, R_{ll} is just given by twice the probability that one B oscillates times the probability that the other B does not change flavour. The behaviour is quite different on the $\Upsilon(4S)$ resonance or at the $B\bar{B}^*$ production threshold, because the $B^0\bar{B}^0$ pairs are produced coherently, i.e. in a state of definite orbital angular momentum (odd/even at the $\Upsilon(4S)/B\bar{B}^*$ threshold). Quantum statistics for spin zero particles requires then an antisymmetric (symmetric) $B^0\bar{B}^0$ wave function for odd (even) orbital angular momentum. Taking this into account,

$$R_{ll} = \begin{cases} x^2/[2(1+x^2)] & [\Upsilon(4S)] \\ x^2(3+x^2)/[2(1+x^2)^2] & [B\bar{B}^* \text{ threshold}] \\ 2\chi(1-\chi) & [\text{LEP}] \end{cases} . \quad (10.18)$$

At the $\Upsilon(4S)$, the lepton like–sign fraction (corrected for leptons coming from B^+B^- pairs) directly measures the mixing transition $B_d^0 \rightarrow \bar{B}_d^0$. However, at higher energies both B_d^0 and B_s^0 are produced, and one measures a combination of their mixing probabilities, weighted by their production fractions: $\bar{\chi} = f_{B_d^0}\chi_{B_d^0} + f_{B_s^0}\chi_{B_s^0}$.

Evidence for a large $B_d^0\text{--}\bar{B}_d^0$ mixing was first reported in 1987 by ARGUS⁹² and later confirmed by CLEO.⁹³ This provided the first indication that the top quark was very heavy. Since then, many experiments have analyzed the mixing probability.^{28,94} The present world–average value of $\chi_{B_d^0}$ from threshold experiments is²⁸

$$\chi_{B_d^0} = 0.151 \pm 0.028, \quad (10.19)$$

which implies $x_{B_d^0} = 0.66 \pm 0.09$. The high–energy measurements are compatible with this number and together they indicate a maximal value for $\chi_{B_s^0} \sim 0.5$, in agreement with the SM expectation

$$\frac{x_{B_s^0}}{x_{B_d^0}} \sim \frac{|V_{ts}|^2}{|V_{td}|^2} \gg 1. \quad (10.20)$$

Unfortunately, χ becomes insensitive to x when mixing is maximal. For instance, $\chi_{B_s^0} > 0.4$ corresponds to the weak limit $x_{B_s^0} > 2$. Time integrated measurements are then not sensitive to the rapid oscillations of the B_s^0 meson.

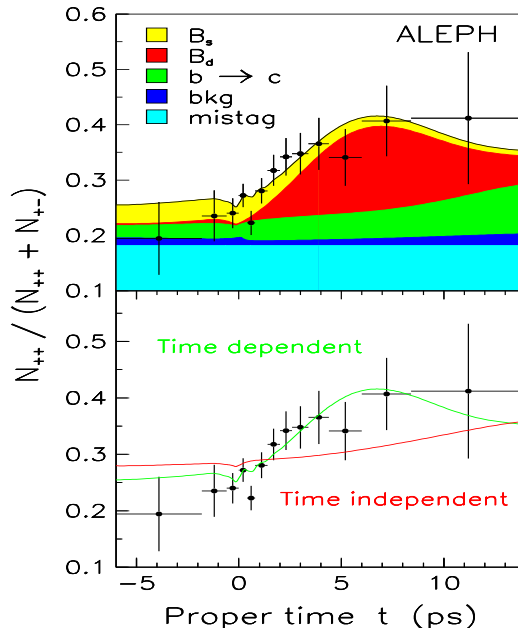


Figure 10: Dilepton like–sign fraction as a function of time from ALEPH.⁹⁵

The LEP experiments have performed explicit measurements of the mixing probability $B_d^0 \rightarrow \bar{B}_d^0$ as a function of time.^{95,96,97} Fig. 10 shows the time–dependent fraction of like–sign leptons measured by ALEPH,⁹⁵ which provides clear evidence of

the oscillatory behaviour. A fit to the time dependence allows to extract $\Delta M_{B_d^0}$. The present LEP average is²⁸

$$\Delta M_{B_d^0} = 0.501 \pm 0.034 \text{ ps}^{-1}. \quad (10.21)$$

Combined with (10.19) and the measured B_d^0 lifetime, this gives the world average²⁸

$$\Delta M_{B_d^0} = 0.462 \pm 0.026 \text{ ps}^{-1}; \quad x_{B_d^0} = 0.76 \pm 0.05. \quad (10.22)$$

The LEP experiments have also searched for a high-frequency component in their fit to the proper-time distribution, trying to pin down the B_s^0 contribution. The present upper limit on the B_s^0 - \bar{B}_s^0 mixing is⁹⁷

$$\Delta M_{B_s^0} > 2.2 \text{ ps}^{-1}, \quad x_{B_s^0} > 3.0, \quad (95\% \text{ CL}). \quad (10.23)$$

10.3. Mixing constraints on the CKM matrix

The calculation of the short-distance box diagrams in Fig. 9 is rather straightforward. Moreover, the leading and next-to-leading gluonic corrections are already known.⁹⁸ Unfortunately, this is not enough to get an accurate prediction for the mixing probability. The main theoretical uncertainty stems from the hadronic matrix element of the $\Delta B = 2$ four-quark operator generated by the box diagrams:

$$\langle \bar{B}^0 | (\bar{b}\gamma^\mu(1 - \gamma_5)d) (\bar{b}\gamma_\mu(1 - \gamma_5)d) | B^0 \rangle \equiv \frac{8}{3} M_B^2 (\sqrt{2} \xi_B)^2. \quad (10.24)$$

The size of this matrix element is characterized through the non-perturbative parameter $\xi_B \equiv f_B \sqrt{B_B}$, which is rather badly known. Present calculations favour the range⁹⁹ $\hat{\xi}_B \equiv \alpha_s(\mu^2)^{-3/23} \xi_B(\mu^2) = 185 \pm 50 \text{ MeV}$ [μ is the renormalization scale]. With $\bar{m}_t = 173 \pm 12 \text{ GeV}$, the measured mixing in (10.22) implies

$$|\mathbf{V}_{td}| = 0.007 \pm 0.002, \quad (10.25)$$

in good agreement with (but more precise than) the value obtained from the unitarity constraint in (9.2). In terms of the (ρ, η) parametrization of Eq. (9.4), this gives

$$\sqrt{(1 - \rho)^2 + \eta^2} = \left| \frac{\mathbf{V}_{td}}{\lambda \mathbf{V}_{cb}} \right| = 0.8 \pm 0.2. \quad (10.26)$$

The same analysis can be applied to the B_s^0 - \bar{B}_s^0 mixing probability. The non-perturbative uncertainties can be reduced to the level of $SU(3)$ breaking corrections through the ratio

$$\frac{\Delta M_{B_s^0}}{\Delta M_{B_d^0}} \approx \frac{M_{B_s^0} \xi_{B_s^0}^2}{M_{B_d^0} \xi_{B_d^0}^2} \left| \frac{\mathbf{V}_{ts}}{\mathbf{V}_{td}} \right|^2 \approx (1.0 \pm 0.2) \times \left| \frac{\mathbf{V}_{ts}}{\mathbf{V}_{td}} \right|^2, \quad (10.27)$$

where we have made the reasonable assumption $(\xi_{B_s}/\xi_{B_d})^2 \approx 1.0 \pm 0.2$. The present bounds on ΔM_{B^0} imply then

$$\left| \frac{\mathbf{V}_{ts}}{\mathbf{V}_{td}} \right| > 1.8 \quad (95\% \text{ CL}). \quad (10.28)$$

This should be compared with the unitarity constraint $|\mathbf{V}_{ts}/\mathbf{V}_{td}| = 4.4 \pm 2.6$.

11. CP–Violation

Since $\delta_{13}(\eta)$ is the only possible source of CP violation, the SM predictions for CP–violating phenomena are quite constrained. Moreover, the CKM mechanism requires several necessary conditions in order to generate an observable CP–violation effect. With only two fermion generations, the quark–mixing mechanism cannot give rise to CP violation; therefore, for CP violation to occur in a particular process, all 3 generations are required to play an active role. In the kaon system, for instance, CP–violation effects can only appear at the one–loop level, where the top quark is present. In addition, all CKM–matrix elements must be non–zero and the quarks of a given charge must be non–degenerate in mass. If any of these conditions were not satisfied, the CKM–phase could be rotated away by a redefinition of the quark fields. CP–violation effects are then necessarily proportional to the product of all CKM angles, and should vanish in the limit where any two (equal–charge) quark masses are taken to be equal. All these necessary conditions can be summarized in a very elegant way as a single requirement¹⁰⁰ on the original quark–mass matrices \mathbf{M}'_u and \mathbf{M}'_d :

$$\text{CP violation} \iff \text{Im} \left\{ \det \left[\mathbf{M}'_u \mathbf{M}'_u{}^\dagger, \mathbf{M}'_d \mathbf{M}'_d{}^\dagger \right] \right\} \neq 0. \quad (11.1)$$

Without performing any detailed calculation, one can make the following general statements on the implications of the CKM mechanism of CP violation:

- Owing to unitarity, for any choice of i, j, k, l (between 1 and 3),

$$\text{Im} \left[\mathbf{V}_{ij} \mathbf{V}_{ik}^* \mathbf{V}_{lk} \mathbf{V}_{lj}^* \right] = \mathcal{J} \sum_{m,n=1}^3 \epsilon_{ilm} \epsilon_{jkn}, \quad (11.2)$$

$$\mathcal{J} = c_{12} c_{23} c_{13}^2 s_{12} s_{23} s_{13} \sin \delta_{13} \approx A^2 \lambda^6 \eta < 10^{-4}. \quad (11.3)$$

Any CP–violation observable involves¹⁰⁰ the product \mathcal{J} . Thus, violations of the CP symmetry are necessarily small.

- In order to have sizeable CP–violating asymmetries $[(\Gamma - \bar{\Gamma})/(\Gamma + \bar{\Gamma})]$, one should look for very suppressed decays, where the decay widths already involve small CKM matrix elements.
- In the SM, CP violation is a low–energy phenomena in the sense that any effect should disappear when the quark–mass difference $m_c - m_u$ becomes negligible.

- B decays are the optimal place for CP–violation signals to show up. They involve small CKM matrix elements and are the lowest–mass processes where the three quark generations play a direct (tree–level) role.

The SM mechanism of CP violation is based in the unitarity of the CKM matrix. Testing the constraints implied by unitarity is then a way to test the source of CP violation. Up to now, the only unitarity relation which has been precisely tested is the one associated with the first row of the CKM matrix; however, only the moduli of the CKM parameters appear in Eq. (9.1), while CP violation has to do with their phases. More interesting are the off–diagonal unitarity conditions:

$$\begin{aligned}
\mathbf{V}_{ud}^* \mathbf{V}_{us} + \mathbf{V}_{cd}^* \mathbf{V}_{cs} + \mathbf{V}_{td}^* \mathbf{V}_{ts} &= 0, \\
\mathbf{V}_{us}^* \mathbf{V}_{ub} + \mathbf{V}_{cs}^* \mathbf{V}_{cb} + \mathbf{V}_{ts}^* \mathbf{V}_{tb} &= 0, \\
\mathbf{V}_{ub}^* \mathbf{V}_{ud} + \mathbf{V}_{cb}^* \mathbf{V}_{cd} + \mathbf{V}_{tb}^* \mathbf{V}_{td} &= 0.
\end{aligned}
\tag{11.4}$$

These relations can be visualized by triangles in a complex plane¹⁰¹ which, owing to Eq. (11.2), have the same area $|\mathcal{J}|/2$. In the absence of CP violation, these triangles would degenerate into segments along the real axis.

In the first two triangles, one side is much shorter than the other two (the Cabibbo suppression factors of the three sides are λ , λ and λ^5 in the first triangle, and λ^4 , λ^2 and λ^2 in the second one). This is the reason why CP effects are so small for K mesons (first triangle), and why certain asymmetries in B_s decays are predicted to be tiny (second triangle).

The third triangle looks more interesting, since the three sides have a similar size of about λ^3 . They are small, which means that the relevant b –decay branching ratios are small, but once enough B mesons would be produced, CP–violation asymmetries are going to be sizeable. This triangle is shown in Fig. 11, where it has been scaled by dividing its sides by $|\mathbf{V}_{cb}^* \mathbf{V}_{cd}|$. In the approximate parametrization (9.4), where $\mathbf{V}_{cb}^* \mathbf{V}_{cd}$ is real, this aligns one side of the triangle along the real axis and makes its length equal to 1; the coordinates of the 3 vertices are then $(0, 0)$, $(1, 0)$ and (ρ, η) . Note that, although the orientation of the triangle in the complex plane is phase–convention dependent, the triangle itself is a physical object: the length of the sides and/or the angles can be directly measured. In fact, we have already determined its sides from the measured ratio $\Gamma(b \rightarrow u)/\Gamma(b \rightarrow c)$ and from B_d^0 – \bar{B}_d^0 mixing:

$$R_b \equiv \left| \frac{\mathbf{V}_{ub}^* \mathbf{V}_{ud}}{\mathbf{V}_{cb}^* \mathbf{V}_{cd}} \right| \approx \left| \frac{\mathbf{V}_{ub}}{\lambda \mathbf{V}_{cb}} \right| \approx \sqrt{\rho^2 + \eta^2} = 0.36 \pm 0.10, \tag{11.5}$$

$$R_t \equiv \left| \frac{\mathbf{V}_{tb}^* \mathbf{V}_{td}}{\mathbf{V}_{cb}^* \mathbf{V}_{cd}} \right| \approx \left| \frac{\mathbf{V}_{td}}{\lambda \mathbf{V}_{cb}} \right| \approx \sqrt{(1 - \rho)^2 + \eta^2} = 0.8 \pm 0.2. \tag{11.6}$$

In principle, the measurement of these two sides, performed through CP–conserving observables, could make possible to establish that CP is violated (assuming unitarity), by showing that they indeed give rise to a triangle and not to a straight line. With the present experimental and theoretical errors, this is however not possible yet.

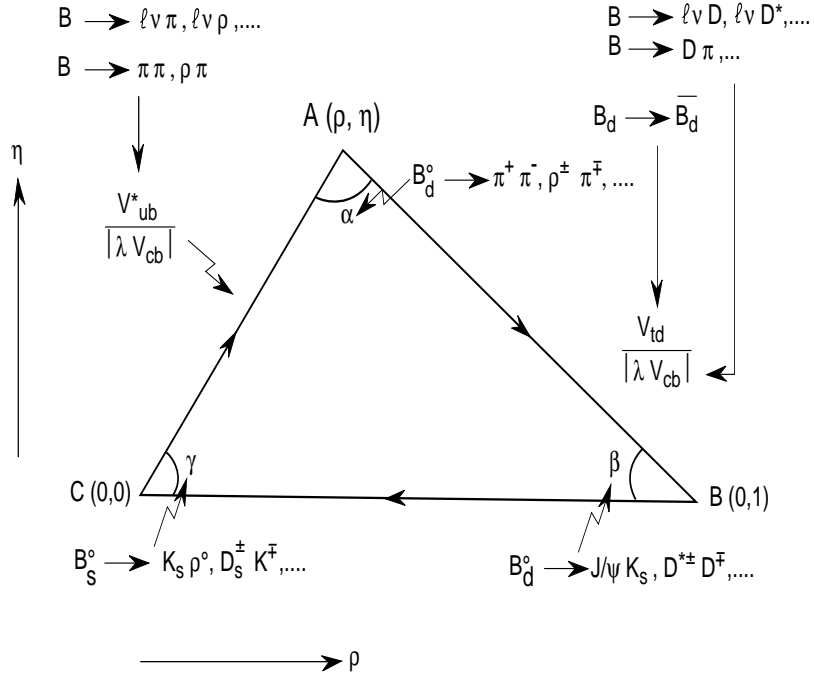


Figure 11: The unitarity triangle. Also shown are various topics in B physics that allow to measure its sides and angles.¹⁰²

11.1. Indirect and Direct CP Violation in the Kaon System

Any observable CP-violation effect is generated by the interference between different amplitudes contributing to the same physical transition. This interference can occur either through meson-antimeson mixing or via final-state interactions, or by a combination of both effects.

The flavour-specific decays $K^0 \rightarrow \pi^- l^+ \nu_l$ and $\bar{K}^0 \rightarrow \pi^+ l^- \bar{\nu}_l$ provide a way to measure the departure of the K^0 - \bar{K}^0 mixing parameter $|p/q|$ from unity. In the SM, $|A(\bar{K}^0 \rightarrow \pi^+ l^- \bar{\nu}_l)| = |A(K^0 \rightarrow \pi^- l^+ \nu_l)|$; therefore,

$$\delta \equiv \frac{\Gamma(K_L \rightarrow \pi^- l^+ \nu_l) - \Gamma(K_L \rightarrow \pi^+ l^- \bar{\nu}_l)}{\Gamma(K_L \rightarrow \pi^- l^+ \nu_l) + \Gamma(K_L \rightarrow \pi^+ l^- \bar{\nu}_l)} = \frac{|p|^2 - |q|^2}{|p|^2 + |q|^2} = \frac{2 \operatorname{Re}(\bar{\varepsilon}_K)}{(1 + |\bar{\varepsilon}_K|^2)}. \quad (11.7)$$

The experimental measurement,⁶ $\delta = (3.27 \pm 0.12) \times 10^{-3}$, implies

$$\operatorname{Re}(\bar{\varepsilon}_K) = (1.63 \pm 0.06) \times 10^{-3}, \quad (11.8)$$

which establishes the presence of *indirect* CP-violation generated by the mixing amplitude.

If the flavour of the decaying meson P is known, any observed difference between the decay rate $\Gamma(P \rightarrow f)$ and its CP conjugate $\Gamma(\bar{P} \rightarrow \bar{f})$ would indicate that CP is directly violated in the decay amplitude. One could study, for instance, CP asymmetries in charged-kaon decays, such as $K^\pm \rightarrow \pi^\pm \pi^0$, where the charge of the final pions clearly identifies the flavour of the decaying kaon (these types of decays are often referred to as self-tagging modes). No positive signal has been reported up to date.

Since at least two interfering amplitudes are needed to generate a CP-violating effect, let us write the amplitudes for the transitions $P \rightarrow f$ and $\bar{P} \rightarrow \bar{f}$ as

$$A[P \rightarrow f] = M_1 e^{i\phi_1} e^{i\alpha_1} + M_2 e^{i\phi_2} e^{i\alpha_2}, \quad (11.9)$$

$$A[\bar{P} \rightarrow \bar{f}] = M_1 e^{-i\phi_1} e^{i\alpha_1} + M_2 e^{-i\phi_2} e^{i\alpha_2}, \quad (11.10)$$

where ϕ_1, ϕ_2 denote weak phases, α_1, α_2 strong final-state phases, and M_1, M_2 the moduli of the matrix elements. The rate asymmetry is given by

$$\frac{\Gamma[P \rightarrow f] - \Gamma[\bar{P} \rightarrow \bar{f}]}{\Gamma[P \rightarrow f] + \Gamma[\bar{P} \rightarrow \bar{f}]} = \frac{-2M_1 M_2 \sin(\phi_1 - \phi_2) \sin(\alpha_1 - \alpha_2)}{|M_1|^2 + |M_2|^2 + 2M_1 M_2 \cos(\phi_1 - \phi_2) \cos(\alpha_1 - \alpha_2)}. \quad (11.11)$$

Thus, to generate a direct-CP asymmetry one needs:

1. Two (at least) interfering amplitudes.
2. Two different weak phases [$\sin(\phi_1 - \phi_2) \neq 0$].
3. Two different strong phases [$\sin(\alpha_1 - \alpha_2) \neq 0$].

Moreover, in order to get a sizeable asymmetry, the two amplitudes M_1 and M_2 should be of comparable size.

In the kaon system, direct CP violation has been searched for in decays of neutral kaons, where K^0 - \bar{K}^0 mixing is also involved. Thus, both direct and indirect CP-violation effects need to be taken into account, simultaneously. Since the $\pi^+\pi^-$ and $2\pi^0$ states are even under CP, only the K_1 state could decay into 2π if CP were conserved. Thus, a CP-violation signal is provided by the ratios:

$$\eta_{+-} \equiv \frac{A(K_L \rightarrow \pi^+\pi^-)}{A(K_S \rightarrow \pi^+\pi^-)} \equiv |\eta_{+-}| e^{i\phi_{+-}} \approx \varepsilon_K + \frac{\varepsilon'_K}{1 + \omega/\sqrt{2}}, \quad (11.12)$$

$$\eta_{00} \equiv \frac{A(K_L \rightarrow \pi^0\pi^0)}{A(K_S \rightarrow \pi^0\pi^0)} \equiv |\eta_{00}| e^{i\phi_{00}} \approx \varepsilon_K - \frac{2\varepsilon'_K}{1 - \sqrt{2}\omega}, \quad (11.13)$$

where [terms quadratic in the small CP-violating quantities have been neglected]

$$\varepsilon_K \equiv \bar{\varepsilon}_K + i\xi_0, \quad \varepsilon'_K \equiv \frac{i}{\sqrt{2}} \omega (\xi_2 - \xi_0), \quad \omega \equiv \frac{\text{Re}(A_2)}{\text{Re}(A_0)} e^{i(\delta_2 - \delta_0)}. \quad (11.14)$$

A_I and δ_I are the decay–amplitudes and strong phase–shifts of isospin $I = 0, 2$ (these are the only two values allowed by Bose symmetry for the final 2π state),

$$A[K^0 \rightarrow (2\pi)_I] \equiv iA_I e^{i\delta_I}, \quad A[\bar{K}^0 \rightarrow (2\pi)_I] \equiv -iA_I^* e^{i\delta_I}, \quad (11.15)$$

and

$$\xi_I \equiv \frac{\text{Im}(A_I)}{\text{Re}(A_I)}. \quad (11.16)$$

The parameter ε_K is related to the indirect CP violation. Note that ε_K is a physical (measurable) phase–convention–independent quantity, while $\bar{\varepsilon}_K$ is not [$\varepsilon_K = \bar{\varepsilon}_K$ in the phase convention $\text{Im}(A_0) = 0$; however, $\text{Re}(\varepsilon_K) = \text{Re}(\bar{\varepsilon}_K)$ in any convention]. Direct CP violation is measured through ε'_K , which is governed by the phase–difference between the two isospin amplitudes. The CP–conserving parameter ω gives the relative size between these two amplitudes; experimentally, one finds a very big enhancement of the $I = 0$ channel with respect to the $I = 2$ one, which is known as the $\Delta I = 1/2$ rule:

$$|\omega| \approx \frac{1}{22}, \quad \delta_2 - \delta_0 = -45^\circ \pm 6^\circ. \quad (11.17)$$

The small size of $|\omega|$ implies a strong suppression of ε'_K .

From the eigenvector equations for K_S and K_L one can easily obtain the relation

$$\bar{\varepsilon}_K \approx e^{i\phi_{SW}} \frac{\text{Im}(M_{12}) - \frac{i}{2}\text{Im}(\Gamma_{12})}{\sqrt{\Delta M_{K^0}^2 + \frac{1}{4}\Delta\Gamma_{K^0}^2}}, \quad (11.18)$$

where⁶ $\Delta M_{K^0} \equiv M_{K_L} - M_{K_S} = (3.510 \pm 0.018) \times 10^{-12}$ MeV, $\Delta\Gamma_{K^0} \equiv \Gamma_{K_L} - \Gamma_{K_S} = -(7.361 \pm 0.010) \times 10^{-12}$ MeV, and

$$\phi_{SW} \equiv \arctan\left(\frac{-2\Delta M_{K^0}}{\Delta\Gamma_{K^0}}\right) = 43.64^\circ \pm 0.15^\circ \quad (11.19)$$

is the so–called superweak phase. Since $\Delta\Gamma_{K^0} \approx -2\Delta M_{K^0}$, one has $\phi_{SW} \approx \pi/4$. Moreover, $\text{Im}(\Gamma_{12})/\text{Re}(\Gamma_{12}) \approx -2\xi_0$ because Γ_{12} is dominated by the $K^0 \rightarrow (2\pi)_{I=0}$ decay mode. Using these relations, one gets the approximate result

$$\varepsilon_K \approx \frac{e^{i\pi/4}}{\sqrt{2}} \left\{ \frac{\text{Im}(M_{12})}{2\text{Re}(M_{12})} + \xi_0 \right\}. \quad (11.20)$$

Notice that $\delta_2 - \delta_0 + \pi/2 \approx \pi/4$, i.e.

$$\varepsilon'_K \approx \frac{e^{i\pi/4}}{\sqrt{2}} |\omega| (\xi_2 - \xi_0). \quad (11.21)$$

Thus, owing to the particular numerical values of the neutral–kaon decay parameters, the phases of ε_K and ε'_K are nearly equal.

The experimental world–averages quoted by the Particle Data Group⁶ are

$$|\eta_{+-}| = (2.269 \pm 0.023) \times 10^{-3}, \quad \phi_{+-} = (44.3 \pm 0.8)^\circ, \quad (11.22)$$

$$|\eta_{00}| = (2.259 \pm 0.023) \times 10^{-3}, \quad \phi_{00} = (43.3 \pm 1.3)^\circ. \quad (11.23)$$

The phases are very close to $\pi/4$, whereas the moduli are equal within errors, showing that indeed $|\varepsilon'_K| \ll |\varepsilon_K|$ as expected from the $|\omega|$ suppression. Moreover, these numbers imply $\text{Re}(\varepsilon_K) \approx 1.63 \times 10^{-3}$, in good agreement with the value (11.8) extracted from semileptonic decays.

The ratio $\varepsilon'_K/\varepsilon_K$ can be determined through the relation

$$\text{Re} \left(\frac{\varepsilon'_K}{\varepsilon_K} \right) \approx \frac{1}{6} \left\{ 1 - \left| \frac{\eta_{00}}{\eta_{+-}} \right|^2 \right\}. \quad (11.24)$$

Two different experiments have recently reported a measurement of this quantity:

$$\text{Re} \left(\frac{\varepsilon'_K}{\varepsilon_K} \right) = \begin{cases} (23.0 \pm 6.5) \times 10^{-4} & [\text{NA31}^{103}] \\ (7.4 \pm 5.9) \times 10^{-4} & [\text{E731}^{104}] \end{cases}. \quad (11.25)$$

The NA31 measurement provides evidence for a non–zero value of $\varepsilon'_K/\varepsilon_K$ (i.e., direct CP violation), with a statistical significance of more than three standard deviations. However, this is not supported by the E731 result, which is compatible with $\varepsilon'_K/\varepsilon_K = 0$, thus with no direct CP violation. The probability for the two results being statistically compatible is only 7.6%.

New experiments with a better sensitivity are required in order to resolve this discrepancy. A next generation of $\varepsilon'_K/\varepsilon_K$ experiments is already under construction at CERN¹⁰⁵ and Fermilab.¹⁰⁶ Moreover, a dedicated ϕ factory (DAΦNE), providing large amounts of tagged K_S , K_L and K^\pm ($\phi \rightarrow K\bar{K}$), is being built at Frascati.¹⁰⁷ The goal of all these experiments is to reach sensitivities better than 10^{-4} .

The CKM mechanism generates CP–violation effects both in the $\Delta S = 2$ $K^0\text{--}\bar{K}^0$ transition (box–diagrams) and in the $\Delta S = 1$ decay amplitudes (penguin diagrams). The theoretical analysis of $K^0\text{--}\bar{K}^0$ mixing is quite similar to the one applied to the B system. This time, however, the charm loop contributions are non–negligible. The main uncertainty stems from the calculation of the hadronic matrix element of the four–quark $\Delta S = 2$ operator, which is usually parametrized through the non–perturbative parameter⁹⁹ $\hat{B}_K \approx 0.4\text{--}0.8$.

The experimental value of ε_K specifies a hyperbola in the (ρ, η) plane. This is shown in Fig. 12, together with the constraints (11.5) and (11.6), which result in the circles centered at $(0, 0)$ and $(1, 0)$, respectively. The final allowed range of values for (ρ, η) is given by the intersection of all constraints.

The theoretical estimate of $\varepsilon'_K/\varepsilon_K$ is much more involved, because ten four–quark operators need to be considered in the analysis and the presence of cancellations

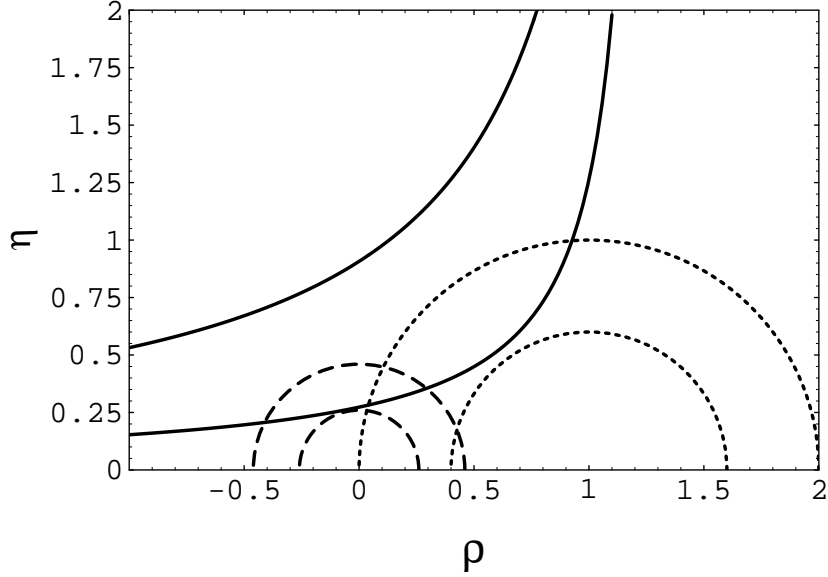


Figure 12: Present constraints on the Unitarity Triangle.

between different contributions tends to amplify the sensitivity to the not very well controlled long-distance effects. For large values of the top-mass, the Z^0 -penguin contributions strongly suppress the expected value of $\varepsilon'_K/\varepsilon_K$, making the final result very sensitive to m_t . The present theoretical estimates^{108,109} range from -3×10^{-4} to 10^{-3} . More theoretical work is needed in order to get firm predictions.

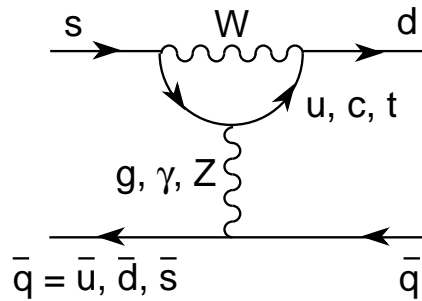


Figure 13: $\Delta S = 1$ penguin diagrams.

11.2. Bottom decays

The flavour-specific decays $B^0 \rightarrow Xl^+\nu_l$ and $\bar{B}^0 \rightarrow Xl^-\bar{\nu}_l$ provide the most direct way to measure the amount of CP violation in the B^0 - \bar{B}^0 mixing matrix. The asymmetry between the number of l^+l^+ and l^-l^- pairs produced in the processes

$e^+e^- \rightarrow B^0\bar{B}^0 \rightarrow l^\pm l^\pm X$ is easily found to be

$$a_{SL} \equiv \frac{N(l^+l^+) - N(l^-l^-)}{N(l^+l^+) + N(l^-l^-)} = \frac{|p/q|^2 - |q/p|^2}{|p/q|^2 + |q/p|^2} \approx 4 \operatorname{Re}(\bar{\varepsilon}_B). \quad (11.26)$$

Unfortunately, this $\Delta B = 2$ asymmetry is expected to be quite tiny in the SM, because $|\Delta\Gamma_{B^0}/\Delta M_{B^0}| \approx |\Gamma_{12}/M_{12}| \sim m_b^2/m_t^2 \ll 1$ and, moreover, there is an additional GIM suppression in the phase $\phi_{\Delta B=2} \equiv \arg(M_{12}/\Gamma_{12}) \sim (m_c^2 - m_u^2)/m_b^2$, implying a value of $|q/p|$ very close to 1. Thus,

$$a_{SL} \leq \begin{cases} 10^{-3} & (B_d^0), \\ 10^{-4} & (B_s^0). \end{cases} \quad (11.27)$$

The observation of an asymmetry a_{SL} at the percent level, would then be a clear indication of new physics beyond the SM.

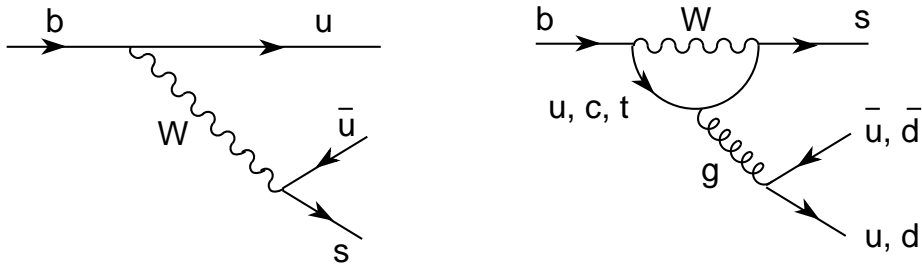


Figure 14: Feynman diagrams contributing to $B^- \rightarrow K^- \rho^0$

Direct CP violation could be established by measuring a non-zero rate asymmetry in B^\pm decays. One example is the decay $B^\pm \rightarrow K^\pm \rho^0$ which proceeds via a tree and a penguin diagram the weak couplings of which are given by $\mathbf{V}_{ub}\mathbf{V}_{us}^* \approx A\lambda^4(\rho - i\eta)$ and $\mathbf{V}_{tb}\mathbf{V}_{ts}^* \approx -A\lambda^2$, respectively.^b Although the penguin contribution is of higher-order in the strong coupling, and suppressed by the loop factor $1/(16\pi^2)$, one could expect both amplitudes to be of comparable size, owing to the additional λ^2 suppression factor of the tree diagram. The needed strong-phase difference can be generated through the absorptive part of the penguin diagram, corresponding to on-shell intermediate particle rescattering.¹¹⁰ Therefore, one could expect a sizeable asymmetry, provided the strong-phase difference is not too small. However, a very large number of B^\pm is required, because the branching ratio is quite suppressed ($\sim 10^{-5}$). Other decay modes such as¹¹¹ $B^\pm \rightarrow K^\pm K_S, K^\pm K^{*0}$ involve the interference between penguin diagrams only and might show sizeable CP-violating asymmetries as well, but the corresponding branching fractions are expected to be even smaller.

^b Since $m_u, m_c \ll M_W$, we can neglect the small quark-mass corrections in the up and charm penguin contributions. These two diagrams then differ in their CKM factors only, and their sum is regulated by the same CKM factor than the top-quark loop, due to the unitarity of \mathbf{V} .

The two interfering amplitudes can also be generated through other mechanisms. For instance, one can have an interplay between two different cascade processes^{112,113} like $B^- \rightarrow D^0 X^- \rightarrow K_S Y^0 X^-$ and $B^- \rightarrow \bar{D}^0 X^- \rightarrow K_S Y^0 X^-$. Another possibility would be an interference between two tree diagrams corresponding to two different decay mechanisms like direct decay (spectator) and weak annihilation.¹¹⁴ Direct CP violation could also be studied in decays of bottom baryons,¹¹⁵ where it could show up as a rate asymmetry and in various decay parameters.

Note that, for all these flavour-specific decays, the necessary presence of strong phases makes very difficult to extract useful information on the CKM factors from their measured CP asymmetries. Nevertheless, the experimental observation of a non-zero CP-violating asymmetry in any of these decay modes would be a major milestone in our understanding of CP-violation phenomena, as it would clearly establish the existence of direct CP violation in the decay amplitudes.

The large B^0 - \bar{B}^0 mixing provides a different way to generate the required CP-violating interference. There are quite a few non-leptonic final states which are reachable both from a B^0 and a \bar{B}^0 . For these flavour non-specific decays the B^0 (or \bar{B}^0) can decay directly to the given final state f , or do it after the meson has been changed to its antiparticle via the mixing process; i.e., there are two different amplitudes, $A(B^0 \rightarrow f)$ and $A(B^0 \rightarrow \bar{B}^0 \rightarrow f)$, corresponding to two possible decay paths. CP-violating effects can then result from the interference of these two contributions.

The time-dependent decay probabilities for the decay of a neutral B meson created at the time $t_0 = 0$ as a pure B^0 (\bar{B}^0) into the final state f ($\bar{f} \equiv CP f$) are (we neglect the tiny $\Delta\Gamma_{B^0}$ corrections):

$$\Gamma[B^0(t) \rightarrow f] \propto \frac{1}{2} e^{-\Gamma_{B^0} t} |A_f|^2 \left\{ [1 + |\bar{\rho}_f|^2] + [1 - |\bar{\rho}_f|^2] \cos(\Delta M_{B^0} t) - 2 \operatorname{Im} \left(\frac{q}{p} \bar{\rho}_f \right) \sin(\Delta M_{B^0} t) \right\}, \quad (11.28)$$

$$\Gamma[\bar{B}^0(t) \rightarrow \bar{f}] \propto \frac{1}{2} e^{-\Gamma_{B^0} t} |\bar{A}_{\bar{f}}|^2 \left\{ [1 + |\rho_{\bar{f}}|^2] + [1 - |\rho_{\bar{f}}|^2] \cos(\Delta M_{B^0} t) - 2 \operatorname{Im} \left(\frac{p}{q} \rho_{\bar{f}} \right) \sin(\Delta M_{B^0} t) \right\}, \quad (11.29)$$

where we have introduced the notation

$$\begin{aligned} A_f &\equiv A[B^0 \rightarrow f], & \bar{A}_{\bar{f}} &\equiv -A[\bar{B}^0 \rightarrow \bar{f}], & \bar{\rho}_f &\equiv \bar{A}_f/A_f, \\ A_{\bar{f}} &\equiv A[B^0 \rightarrow \bar{f}], & \bar{A}_f &\equiv -A[\bar{B}^0 \rightarrow f], & \rho_{\bar{f}} &\equiv A_{\bar{f}}/\bar{A}_{\bar{f}}. \end{aligned} \quad (11.30)$$

CP invariance demands the probabilities of CP conjugate processes to be identical. Thus, CP conservation requires $A_f = \bar{A}_{\bar{f}}$, $A_{\bar{f}} = \bar{A}_f$, $\bar{\rho}_f = \rho_{\bar{f}}$ and $\operatorname{Im}(\frac{q}{p} \bar{\rho}_f) = \operatorname{Im}(\frac{p}{q} \rho_{\bar{f}})$. Violation of any of the first three equalities would be a signal of direct CP violation. The fourth equality tests CP violation generated by the interference of the direct decay $B^0 \rightarrow f$ and the mixing-induced decay $B^0 \rightarrow \bar{B}^0 \rightarrow f$.

To observe any CP-violating asymmetry, one needs to distinguish between B^0 and \bar{B}^0 decays. However, a final state f that is common to both B^0 and \bar{B}^0 decays cannot reveal by itself whether it came from a B^0 or a \bar{B}^0 . Therefore, one needs independent information on the flavour identity of the decaying neutral B meson. Since beauty hadrons are always produced in pairs, one can use for instance the flavour-specific decays of one B to *tag* the flavour of the companion B .

An obvious example of final states f which can be reached both from the B^0 and the \bar{B}^0 are CP eigenstates; i.e., states such that $\bar{f} = \zeta_f f$ ($\zeta_f = \pm 1$). The ratios $\bar{\rho}_f$ and $\rho_{\bar{f}}$ depend in general on the underlying strong dynamics. However, for CP self-conjugate final states, all dependence on the strong interaction disappears^{112,113} if only one weak amplitude contributes to the $B^0 \rightarrow f$ and $\bar{B}^0 \rightarrow f$ transitions. In this case, we can write the decay amplitude as $A_f = M e^{i\phi_D} e^{i\delta_s}$, where $M = M^*$, ϕ_D is the phase of the weak decay amplitude and δ_s is the strong phase associated with final-state interactions. It is easy to check that the ratios $\bar{\rho}_f$ and $\rho_{\bar{f}}$ are then given by ($A_{\bar{f}} = M \zeta_f e^{i\phi_D} e^{i\delta_s}$, $\bar{A}_f = M \zeta_f e^{-i\phi_D} e^{i\delta_s}$, $\bar{A}_{\bar{f}} = M e^{-i\phi_D} e^{i\delta_s}$)

$$\rho_{\bar{f}} = \bar{\rho}_f^* = \zeta_f e^{2i\phi_D}. \quad (11.31)$$

The unwanted effect of final-state interactions cancels out completely from these two ratios. Moreover, $\rho_{\bar{f}}$ and $\bar{\rho}_f$ simplify in this case to a single weak phase, associated with the underlying weak quark transition.

Since $|\rho_f| = |\bar{\rho}_f| = 1$, the time-dependent decay probabilities become much simpler. In particular, there is no longer any dependence on $\cos(\Delta M_{B^0} t)$. Moreover, for B mesons $|\Gamma_{12}/M_{12}| \ll 1$, implying

$$\frac{q}{p} \approx \sqrt{\frac{M_{12}^*}{M_{12}}} \approx \frac{\mathbf{V}_{tb}^* \mathbf{V}_{tq}}{\mathbf{V}_{tb} \mathbf{V}_{tq}^*} \equiv e^{-2i\phi_M}. \quad (11.32)$$

Here $q \equiv d, s$ stands for B_d^0, B_s^0 . Therefore, the mixing ratio q/p is also given by a known weak phase, and the coefficients of the sinusoidal terms in the time-dependent decay amplitudes are then fully known in terms of CKM mixing angles only:

$$\text{Im} \left(\frac{p}{q} \rho_{\bar{f}} \right) \approx -\text{Im} \left(\frac{q}{p} \bar{\rho}_f \right) \approx \zeta_f \sin [2(\phi_M + \phi_D)] \equiv \zeta_f \sin (2\Phi). \quad (11.33)$$

The time-dependent decay rates are finally given by

$$\Gamma[B^0(t) \rightarrow f] = \Gamma[B^0 \rightarrow f] e^{-\Gamma_{B^0} t} \{1 + \zeta_f \sin(2\Phi) \sin(\Delta M_{B^0} t)\}, \quad (11.34)$$

$$\Gamma[\bar{B}^0(t) \rightarrow \bar{f}] = \Gamma[\bar{B}^0 \rightarrow \bar{f}] e^{-\Gamma_{B^0} t} \{1 - \zeta_f \sin(2\Phi) \sin(\Delta M_{B^0} t)\}. \quad (11.35)$$

In this ideal case, the time-dependent CP-violating decay asymmetry

$$\frac{\Gamma[B^0(t) \rightarrow f] - \Gamma[\bar{B}^0(t) \rightarrow \bar{f}]}{\Gamma[B^0(t) \rightarrow f] + \Gamma[\bar{B}^0(t) \rightarrow \bar{f}]} = \zeta_f \sin(2\Phi) \sin(\Delta M_{B^0} t) \quad (11.36)$$

provides a direct and clean measurement of the CKM parameters.¹¹⁶ Integrating over all decay times yields

$$\int_0^\infty dt \Gamma[B^0(t) \rightarrow f] \propto 1 \mp \zeta_f \sin(2\Phi) \frac{x}{1+x^2}. \quad (11.37)$$

For B_d^0 mesons the mixing term $x_{B_d^0}/(1+x_{B_d^0}^2)$ only suppresses the observable asymmetry by a factor of about two. For B_s^0 mesons, however, the large $B_s^0-\bar{B}_s^0$ mixing would lead to a huge dilution of the CP asymmetry. The measurement of the time-dependence is then a crucial requirement for observing CP-violating asymmetries with B_s^0 mesons.

In e^+e^- machines, running near the $B^0\bar{B}^0$ production threshold, one needs to take also into account the oscillation of the *tagging* meson. The observable time-dependent asymmetry takes then the form

$$\frac{\Gamma[(B^0\bar{B}^0)_{C=\mp} \rightarrow f + (l^-\bar{\nu}_l X^+)] - \Gamma[(B^0\bar{B}^0)_{C=\mp} \rightarrow f + (l^+\nu_l X^-)]}{\Gamma[(B^0\bar{B}^0)_{C=\mp} \rightarrow f + (l^-\bar{\nu}_l X^+)] + \Gamma[(B^0\bar{B}^0)_{C=\mp} \rightarrow f + (l^+\nu_l X^-)]} = \zeta_f \sin(2\Phi) \sin[\Delta M_{B^0}(t \mp \bar{t})], \quad (11.38)$$

where the B flavour has been assumed to be *tagged* through the semileptonic decay, and t (\bar{t}) denotes the time of decay into f (l^\pm). Note that for $C = -1$ the asymmetry vanishes if t and \bar{t} are treated symmetrically. A measurement of at least the sign of $\Delta t \equiv t - \bar{t}$ is necessary to detect CP violation in this case. This is the main reason for building asymmetric B factories.

Decay	CKM factor (Direct)	CKM factor (Penguin)	Exclusive channels	Φ
$\bar{b} \rightarrow \bar{c}c\bar{s}$	$A\lambda^2$	$-A\lambda^2$	$B_d^0 \rightarrow J/\psi K_S, J/\psi K_L$ $B_s^0 \rightarrow D_s^+ D_s^-, J/\psi \eta$	β 0
$\bar{b} \rightarrow \bar{s}s\bar{s}$	–	$-A\lambda^2$	$B_d^0 \rightarrow K_S \phi, K_L \phi$	β
$\bar{b} \rightarrow \bar{d}d\bar{s}$	–	$-A\lambda^2$	$B_s^0 \rightarrow K_S K_S, K_L K_L$	0
$\bar{b} \rightarrow \bar{c}c\bar{d}$	$-A\lambda^3$	$A\lambda^3(1 - \rho - i\eta)$	$B_d^0 \rightarrow D^+ D^-, J/\psi \pi^0$ $B_s^0 \rightarrow J/\psi K_S, J/\psi K_L$	$\approx \beta$ 0
$\bar{b} \rightarrow \bar{u}u\bar{d}$	$A\lambda^3(\rho + i\eta)$	$A\lambda^3(1 - \rho - i\eta)$	$B_d^0 \rightarrow \pi^+ \pi^-, \rho^0 \pi^0, \omega \pi^0$ $B_s^0 \rightarrow \rho^0 K_S, \omega K_S, \pi^0 K_S,$ $\rho^0 K_L, \omega K_L, \pi^0 K_L$	$\approx \beta + \gamma$ $\approx \gamma$
$\bar{b} \rightarrow \bar{s}s\bar{d}$	–	$A\lambda^3(1 - \rho - i\eta)$	$B_d^0 \rightarrow K_S K_S, K_L K_L$ $B_s^0 \rightarrow K_S \phi, K_L \phi$	0 $-\beta$

Table 2: CKM factors and relevant angle Φ for some B -decays into CP-eigenstates.

We have assumed up to now that there is only one amplitude contributing to the given decay process. Unfortunately, this is usually not the case. If several decay amplitudes with different weak and strong phases contribute, $|\bar{\rho}_f| \neq 1$, and the interference term will depend both on the CKM mixing parameters and on the strong dynamics embodied in the ratio $\bar{\rho}_f$.

The leading contributions to $\bar{b} \rightarrow \bar{q}'q'\bar{q}$ decay amplitudes are either *direct* (Fermi) or generated by gluon exchange (penguin). Although of higher order in the strong coupling constant, penguin amplitudes are logarithmically enhanced, due to the virtual W -loop, and are potentially competitive. Table 2 contains the CKM factors associated with the direct and penguin diagrams for different B -decay modes into CP-eigenstates. Also shown is the relevant angle Φ . In terms of CKM elements, the angles α , β and γ are:

$$\alpha \equiv \arg \left[-\frac{\mathbf{V}_{td}\mathbf{V}_{tb}^*}{\mathbf{V}_{ud}\mathbf{V}_{ub}^*} \right], \quad \beta \equiv \arg \left[-\frac{\mathbf{V}_{cd}\mathbf{V}_{cb}^*}{\mathbf{V}_{td}\mathbf{V}_{tb}^*} \right], \quad \gamma \equiv \arg \left[-\frac{\mathbf{V}_{ud}\mathbf{V}_{ub}^*}{\mathbf{V}_{cd}\mathbf{V}_{cb}^*} \right], \quad (11.39)$$

which correspond to the angles of the unitarity triangle in Fig. 11 ($\alpha + \beta + \gamma = \pi$).

The $\bar{b} \rightarrow \bar{c}c\bar{s}$ quark decays are theoretically unambiguous¹¹⁷: the direct and penguin amplitudes have the same weak phase $\Phi = \beta$ (0), for B_d^0 (B_s^0). Ditto for $\bar{b} \rightarrow \bar{s}s\bar{s}$ and $\bar{b} \rightarrow \bar{d}d\bar{s}$, where only the penguin mechanism is possible. The same is true for the Cabibbo-suppressed $\bar{b} \rightarrow \bar{s}s\bar{d}$ mode, which only gets contribution from the penguin diagram; the B_d^0 (B_s^0) phases are 0 ($-\beta$) in this case. The $\bar{b} \rightarrow \bar{c}c\bar{d}$ and $\bar{b} \rightarrow \bar{u}u\bar{d}$ decay modes are not so simple; the two decay mechanisms have the same Cabibbo suppression (λ^3) and different weak phases, but the penguin amplitudes are down by $(\alpha_s/6\pi) \ln(m_W/m_b) \approx 3\%$: these decay modes can be used as approximate measurements of the CKM factors. We have not considered doubly Cabibbo-suppressed decay amplitudes, such as $\bar{b} \rightarrow \bar{u}u\bar{s}$, for which penguin effects can be important and spoil the simple estimates based on the direct decay mechanism.

Presumably the most realistic channels for the measurement of the angles $\Phi = (\beta, \alpha, \gamma)$ are $B_d^0 \rightarrow J/\psi K_S$, $B_d^0 \rightarrow \pi^+\pi^-$ ($\beta+\gamma = \pi-\alpha$) and $B_s^0 \rightarrow \rho^0 K_S$, respectively. The first of these processes is no doubt the one with the cleanest signature and the most tractable background.¹¹⁸ The last process has the disadvantage of requiring a B_s^0 meson and, moreover, its branching ratio is expected to be very small because the *direct* decay amplitude is colour suppressed, leading presumably to a much larger penguin contamination; thus, the determination of γ , through this decay mode looks a quite formidable task.

The decay modes where $\Phi = 0$ are useless for making a determination of the CKM factors. However, some of them provide a very interesting test of the SM, because the prediction that no CP-asymmetry should be seen is very clean. Any detected CP-violating signal would be a clear indication of new physics.

Many other decay modes of B mesons can be used to get information on the CKM factors responsible for CP violation phenomena. A summary, including alternative

ways of measuring γ , can be found in Ref. 102.

12. Rare Decays

Rare decays of K and B mesons are a useful tool to improve our understanding of the interplay among electromagnetic, weak and strong interactions. Decays such as $K \rightarrow \pi\nu\bar{\nu}$ or $B \rightarrow X_s\nu\bar{\nu}$, where QCD corrections can be easily estimated, could provide clean measurements of the relevant CKM factors. CP-violating signals can be looked for in the decays $K_L \rightarrow \pi^0\nu\bar{\nu}$ and $K_L \rightarrow \pi^0l^+l^-$. Other higher-order weak decays like $K_L \rightarrow \mu^+\mu^-$, $K_L \rightarrow \pi^0\gamma\gamma$, $B \rightarrow X_s\gamma$, $B \rightarrow X_sl^+l^-$ or $B \rightarrow l^+l^-$ can be used to make interesting tests of the SM. A detailed discussion of rare decays can be found in Refs. 20, 21, 119, 120 and 121.

13. Summary

The flavour structure of the SM is one of the main pending questions in our understanding of weak interactions. Although we do not know the reason of the observed family replication, we have learned experimentally that the number of SM generations is just three (and no more). Therefore, we must study as precisely as possible the few existing flavours, to get some hints on the dynamics responsible for their observed structure.

The SM imposes two basic constraints on flavour-changing transitions: the universality of the charged-current interactions (the same gauge coupling g for all fermions) and the unitarity of the quark-mixing matrix \mathbf{V} . The empirical verification of these two properties is one of the main motivations to perform a precise experimental investigation of flavour-changing processes.

Since quarks are confined within hadrons, the theoretical analysis of hadronic weak decays requires a good understanding of strong interaction effects. In these lectures, we have discussed a few selected processes where our control on the QCD interplay is good enough to allow a meaningful determination of CKM parameters. Many more weak decays are available for a comprehensive phenomenological study, which could bring precious additional information on the underlying quark couplings, provided our present understanding of strong interactions is improved in a significant way. Obviously, a good sample of measured decays would help to discriminate among different theoretical models and obtain more reliable predictions. Thus, accurate experimental analyses of weak transitions offer the possibility to test both the electroweak and strong interactions.

The SM incorporates a mechanism to generate CP violation, through the single phase naturally occurring in the CKM matrix. This mechanism, deeply rooted into the unitarity structure of \mathbf{V} , implies very specific requirements for CP violation to show up, which should be tested in appropriate experiments. The tiny violation of

the CP symmetry observed in the kaon system, can be parametrized through the CKM phase; however, we do not have yet an experimental verification of the CKM mechanism. Moreover, a fundamental explanation of the origin of this phenomena is still lacking.

In the SM, CP violation is associated with a charged-current interaction with changes the quark flavour in a very definite way: $u_i \rightarrow d_j W^+$, $d_j \rightarrow u_i W^-$. Therefore, CP should be directly violated in many ($\Delta S = 1$, $\Delta D = 1$, $\Delta B = 1$) decay processes without any relation with meson-antimeson mixing. Although the quantitative predictions are often uncertain, owing to the not so-well understood long-distance strong-interaction dynamics, the experimental observation of a non-zero asymmetry in any self-tagging decay mode would be a major achievement, as it would clearly establish the existence of direct CP violation in the decay amplitudes.

The observation of CP-violating asymmetries with neutral B mesons, would allow to independently measure the angles of the unitarity triangle, providing an overconstrained determination of the CKM matrix. If the measured sides and angles turn out to be consistent with a geometrical triangle, we would have a beautiful test of the CKM unitarity, providing strong support to the SM mechanism of CP violation. On the contrary, any deviation from a triangular shape would be a clear proof that new physics is needed to understand CP-violating phenomena.

The dynamics of flavour is a broad and fascinating subject, which is closely related to the so far untested scalar sector of the SM. The experimental verification of the SM predictions is a very important challenge for future experiments. Large surprises may well be discovered, probably giving the first hints of new physics and offering clues to the problems of fermion-mass generation, quark mixing and family replication.

Acknowledgements

I would like to thank the organizers for the charming atmosphere of this meeting. I am also grateful to V. Giménez, J. Prades and E. de Rafael for reading the manuscript. This work has been supported by CICYT (Spain) under grant No. AEN-93-0234.

References

1. A. Pich, *The Standard Model of Electroweak Interactions*, Proc. XXII International Winter Meeting on Fundamental Physics: *The Standard Model and Beyond* (Jaca, 7–11 February 1994), eds. J.A. Villar and A. Morales (Editions Frontières, Gif-sur-Yvette, 1995), p. 1 [hep-ph/9412274].
2. A. Pich, *Quantum Chromodynamics*, Proc. 1994 European School of High-Energy Physics (Sorrento, 1994), eds. N. Ellis and M.B. Gavela, CERN Report CERN 95-04 (Geneva, 1995), p. 157 [hep-ph/9505231].
3. N. Cabibbo, *Phys. Rev. Lett.* **10** (1963) 531.

4. M. Kobayashi and T. Maskawa, *Progr. Theor. Phys.* **42** (1973) 652.
5. S.L. Glashow, J. Iliopoulos and L. Maiani, *Phys. Rev.* **D2** (1970) 1285.
6. Particle Data Group, *Review of Particle Properties*, *Phys. Rev.* **D50** (1994) 1173, and 1995 off-year partial update [URL:<http://pdg.lbl.gov/>].
7. J.Z. Bai *et al* (BES), *Phys. Rev.* **D** to appear [SLAC-PUB-95-6930].
8. J. Gasser and H. Leutwyler, *Phys. Rep.* **87** (1982) 77.
9. H. Leutwyler, *Nucl. Phys.* **B337** (1990) 108.
10. J. Bijnens, J. Prades and E. de Rafael, *Phys. Lett.* **B348** (1995) 226.
11. M. Jamin and M. Münz, *Z. Phys.* **C66** (1995) 633.
12. S. Narison, *QCD Spectral Sum Rules*, Lecture Notes in Physics, Vol. 26 (World Scientific, Singapore, 1989; *Phys. Lett.* **B341** (1994) 73; *Nucl. Phys. B (Proc. Suppl.)* **39B,C** (1995) 446.
13. K.G. Chetyrkin *et al*, *Phys. Rev.* **D51** (1995) 5090.
14. C.R. Allton *et al*, *Nucl. Phys.* **B431** (1994) 667.
15. C.T.H. Davies *et al*, *Phys. Rev. Lett.* **73** (1994) 2654.
16. S. Titard and F.J. Yndurain, *Phys. Rev.* **D49** (1994) 6007.
17. F. Abe *et al* (CDF), *Phys. Rev. Lett.* **74** (1995) 2626; *Phys. Rev.* **D52** (1995) 2605; *Phys. Rev.* **D51** (1995) 4623.
18. S. Abachi *et al* (D0), *Phys. Rev. Lett.* **74** (1995) 2632; *Phys. Rev.* **D52** (1995) 4877.
19. D. Buskulic *et al* (ALEPH), *Phys. Lett.* **B349** (1995) 585.
20. A. Pich, *Chiral Perturbation Theory*, *Rep. Prog. Phys.* **58** (1995) 563.
21. G. Ecker, *Chiral Perturbation Theory*, *Prog. Part. Nucl. Phys.* **35** (1995) 1.
22. R. Tarrach, *Nucl. Phys.* **B183** (1981) 384.
23. N. Gray *et al*, *Z. Phys.* **C48** (1990) 673.
24. T. Kinoshita and A. Sirlin, *Phys. Rev.* **113** (1959) 1652.
25. A. Pich, *Tau Physics*, in *Heavy Flavours* (second edition), eds. A.J. Buras and M. Lindner, Advanced Series on Directions in High Energy Physics – Vol. 10 (World Scientific, Singapore, 1996).
26. J.D. Richman and P.R. Burchat, *Rev. Mod. Phys.* to appear [University of California Preprint No. UCSB-HEP-95-08].
27. Y. Kubota *et al* (CLEO), Preprint CLNS 95/1363.
28. T.E. Browder and K. Honscheid, *Prog. Part. Nucl. Phys.* **35** (1995) 81.
29. E. Noether, *Nach. Ges. Wiss. Göttingen* (1918) 171;
J. Rosen, *Ann. Phys., NY* **69** (1972) 349.
30. J. Goldstone, *Nuovo Cimento* **19** (1961) 154.
31. W.J. Marciano, *Ann. Rev. Nucl. Part. Sci.* **41** (1991) 469.
32. J.C. Hardy *et al*, *Nucl. Phys.* **A509** (1990) 429.
33. I.S. Towner, *Nucl. Phys.* **A540** (1992) 478.
34. F.C. Barker, *Nucl. Phys.* **A540** (1992) 501.
35. W.J. Marciano and A. Sirlin, *Phys. Rev. Lett.* **56** (1986) 22.

36. A. Sirlin and R. Zucchini, *Phys. Rev. Lett.* **57** (1986) 1994.
37. A. Sirlin, *Phys. Rev.* **D35** (1987) 3423.
38. W. Jaus and G. Rasche, *Phys. Rev.* **D35** (1987) 3420; **D41** (1990) 166.
39. J. Gasser and H. Leutwyler, *Ann. Phys., NY* **158** (1984) 142.
40. M. Ademollo and R. Gatto, *Phys. Rev. Lett.* **13** (1964) 264.
41. R.E. Behrends and A. Sirlin, *Phys. Rev. Lett.* **4** (1960) 186.
42. J. Gasser and H. Leutwyler, *Nucl. Phys.* **B250** (1985) 465; 517; 539.
43. H. Leutwyler and M. Roos, *Z. Phys.* **C25** (1984) 91.
44. J.F. Donoghue, B.R. Holstein and S.W. Klimt, *Phys. Rev.* **D35** (1987) 934.
45. H. Abramowicz *et al* , *Z. Phys.* **C15** (1982) 19.
46. A. Bean *et al* (CLEO), *Phys. Lett.* **B317** (1993) 647.
47. M.S. Alam *et al* (CLEO), *Phys. Rev. Lett.* **71** (1993) 1311;
F. Butler *et al* (CLEO), *Phys. Rev.* **D52** (1995) 2656.
48. A. Pich, *Perspectives on Tau-Charm Factory Physics*, Proc. 3rd Workshop on the Tau–Charm Factory (Marbella, Spain, 1993), ed. J. Kirkby and R. Kirkby (Editions Frontières, Gif-sur-Yvette, 1994) 767.
49. N. Isgur and M. Wise, *Phys. Lett.* **B232** (1989) 113; **B237** (1990) 527.
50. B. Grinstein, *Nucl. Phys.* **B339** (1990) 253.
51. E. Eichten and B. Hill, *Phys. Lett.* **B234** (1990) 511.
52. H. Georgi, *Phys. Lett.* **B240** (1990) 447.
53. M. Wirbel, B. Stech and M. Bauer, *Z. Phys.* **C29** (1985) 637; **34** (1987) 103.
54. B. Grinstein, *Ann. Rev. Nucl. Part. Sci.* **42** (1992) 101; *An Introduction to Heavy Mesons*, Lectures at the 6th Mexical School of Particles and Fields (Villahermosa, 1994) [hep-ph/9508227].
55. M. Neubert, *Phys. Rep.* **245** (1994) 259; *Heavy Quark Masses, Mixing Angles and Spin–Flavour Symmetry*, Proc. TASI’93 (Boulder, Colorado, 1993) p. 125.
56. M. Wise, *Heavy Flavor Theory: Overview*, Proc. 16th Int. Symposium on Lepton and Photon Interactions, AIP Conference Proceedings No. 302, ed. P. Drell and D. Rubin (AIP, New York, 1994) p. 253.
57. M. Neubert, *Phys. Lett.* **B264** (1991) 455.
58. M. Luke, *Phys. Lett.* **B252** (1990) 447.
59. J.E. Paschalis and G.J. Gounaris, *Nucl. Phys.* **B222** (1983) 473.
60. F.E. Close, G.J. Gounaris and J.E. Paschalis, *Phys. Lett.* **B149** (1984) 209.
61. M.B. Voloshin and M.A. Shifman, *Sov. J. Nucl. Phys.* **45** (1987) 463; **47** (1988) 511.
62. H.D. Politzer and M.B. Wise, *Phys. Lett.* **B206** (1988) 681; **208** (1988) 504.
63. A.F. Falk and B. Grinstein, *Phys. Lett.* **B247** (1990) 406.
64. X. Ji and M.J. Musolf, *Phys. Lett.* **B257** (1991) 409.
65. D.J. Broadhurst and A.G. Grozin, *Phys. Lett.* **B267** (1991) 105.
66. M. Neubert, *Phys. Rev.* **D46** (1992) 2212; **D51** (1995) 5924;
Nucl. Phys. **B371** (1992) 149; *Phys. Lett.* **B341** (1995) 367.

67. A.F. Falk and M. Neubert, *Phys. Rev.* **D47** (1993) 2965; 2982.
68. T. Mannel, *Phys. Rev.* **D50** (1994) 428.
69. M. Shifman, N.G. Uraltsev and A. Vainshtein, *Phys. Rev.* **D51** (1995) 2217.
70. M. Neubert, *Phys. Lett.* **B338** (1994) 84.
71. M. Neubert, *Heavy Flavour Physics*, Proc. 17th International Conference on Lepton-Photon Interactions (Beijing, 1995) [hep-ph/9511409].
72. H. Albrecht *et al* (ARGUS), *Z. Phys.* **C57** (1993) 533.
73. B. Barish *et al* (CLEO), *Phys. Rev.* **D51** (1995) 1041.
74. D. Buskulic *et al* (ALEPH), *Phys. Lett.* **B359** (1995) 236.
75. D. Bloch *et al* (DELPHI), DELPHI 95-110 PHYS 545 (1995).
76. Y. Nir, *Phys. Lett.* **B221** (1989) 184.
77. M. Luke, M.J. Savage and M.B. Wise, *Phys. Lett.* **B343** (1995) 329; **B345** (1995) 301.
78. P. Ball, M. Beneke and V.M. Braun, *Nucl. Phys.* **B452** (1995) 563; *Phys. Rev.* **D52** (1995) 3929.
79. P. Ball and U. Nierste, *Phys. Rev.* **D50** (1994) 5841.
80. I.I. Bigi, N.G. Uraltsev and A.I. Vainshtein, *Phys. Lett.* **B293** (1992) 430 [E: **B297** (1993) 477].
81. I.I. Bigi *et al*, *Phys. Rev. Lett.* **71** (1993) 496.
82. B. Blok *et al*, *Phys. Rev.* **D49** (1994) 3356 [E: **D50** (1994) 3572].
83. A.V. Manohar and M.B. Wise, *Phys. Rev.* **D49** (1994) 1310.
84. J. Bartelt *et al* (CLEO), *Phys. Rev. Lett.* **71** (1993) 4111;
R. Fulton *et al* (CLEO) *Phys. Rev. Lett.* **64** (1990) 16.
85. H. Albrecht *et al* (ARGUS), *Phys. Lett.* **B255** (1991) 297.
86. R. Ammar *et al* (CLEO), CLEO CONF 95-09 (1995).
87. N. Isgur *et al*, *Phys. Rev.* **D39** (1989) 799.
88. F. Abe *et al* (CDF), FERMILAB-CONF-95-237-E (1995).
89. L. Wolfenstein, *Phys. Rev. Lett.* **51** (1983) 1945.
90. T. Inami and C.S. Lim, *Progr. Theor. Phys.* **65** (1981) 297.
91. M.K. Gaillard and B.W. Lee, *Phys. Rev.* **D10** (1974) 897.
92. H. Albrecht *et al* (ARGUS), *Phys. Lett.* **B192** (1987) 245.
93. M. Artuso *et al* (CLEO), *Phys. Rev. Lett.* **62** (1989) 2233.
94. R. Forty, these proceedings.
95. D. Buskulic *et al* (ALEPH), *Phys. Lett.* **B322** (1994) 441; **B313** (1993) 498.
96. P. Abreu *et al* (DELPHI), *Phys. Lett.* **B338** (1994) 409.
97. R. Akers *et al* (OPAL), *Phys. Lett.* **B336** (1994) 585; **B327** (1994) 411; *Z. Phys.* to appear [CERN PPE-95-12].
98. A.J. Buras, M. Jamin and P.H. Weisz, *Nucl. Phys.* **B347** (1990) 491.
99. A. Pich and J. Prades, *Phys. Lett.* **B346** (1995) 342.
100. C. Jarlskog, *Phys. Rev. Lett.* **55** (1985) 1039; *Z. Phys.* **C29** (1985) 491.
101. L.-L. Chau and W.-Y. Keung, *Phys. Rev. Lett.* **53** (1984) 1802;

- J.D. Bjorken, *Phys. Rev.* **D39** (1989) 1396;
 C. Jarlskog and R. Stora, *Phys. Lett.* **B208** (1988) 268;
 J.L. Rosner, A.I. Sanda and M.P. Schmidt, Proc. Workshop on High Sensitivity Beauty Physics (Fermilab, 1987), ed. A. J. Slaughter *et al*, p. 165.
102. R. Aleksan *et al*, *CP Violation in the B Meson System and Prospects at an Asymmetric B Meson Factory*, Proc. of the ECFA Workshop on a European B–Meson Factory, ed. R. Aleksan and A. Ali, ECFA 93-151.
103. G.D. Barr *et al* (NA31), *Phys. Lett.* **B317** (1993) 233;
 H. Burkhardt *et al*, *Phys. Lett.* **B206** (1988) 169.
104. L.K. Gibbons *et al* (E731), *Phys. Rev. Lett.* **70** (1993) 1203.
105. G. Baar *et al*, Report CERN/SPSC/90-22 (1990).
106. K. Arisaka *et al*, Proposal E832 (1990).
107. *The Second DAΦNE Physics Handbook*, eds. L. Maiani, G. Pancheri and N. Paver (Frascati, 1995).
108. A.J. Buras, M. Jamin and M.E. Lautenbacher, *Nucl. Phys.* **B408** (1993) 209.
109. M. Ciuchini *et al*, *Z. Phys.* **C68** (1995) 239; *Phys. Lett.* **B301** (1993) 263.
110. M. Bander, D. Silverman and A. Soni, *Phys. Rev.* **43** (1979) 242.
111. J.M. Gérard and W.S. Hou, *Phys. Lett.* **B253** (1991) 478; *Phys. Rev.* **D43** (1991) 2909.
112. A. Carter and A.I. Sanda, *Phys. Rev. Lett.* **45** (1980) 952; *Phys. Rev.* **D23** (1981) 1567.
113. I.I. Bigi and A.I. Sanda, *Nucl. Phys.* **B193** (1981) 85.
114. J. Bernabéu and C. Jarlskog, *Z. Phys.* **C8** (1981) 233.
115. J.D. Bjorken, *Nucl. Phys. B (Proc. Suppl.)* **11** (1989) 325;
 I.I. Bigi and B. Stech, Proc. of the Workshop on High Sensitivity Beauty Physics (Fermilab, 1987), ed. A.J. Slaughter *et al*, p. 239;
 I. Dunietz, *Z. Phys.* **C56** (1992) 129.
116. P. Krawczyk *et al*, *Nucl. Phys.* **B307** (1988) 19.
117. D. London and R.D. Peccei, *Phys. Lett.* **B223** (1989) 257.
118. T. Nakada, these proceedings.
119. G. D’Ambrosio *et al*, *Radiative Non-Leptonic Kaon Decays*, Ref. 107, p. 265.
120. E. de Rafael, *Chiral Lagrangians and Kaon CP-Violation*, in *CP Violation and the Limits of the Standard Model*, Proc. TASI’94, ed. J.F. Donoghue (World Scientific, Singapore, 1995).
121. G. Buchalla, A.J. Buras and M.E. Lautenbacher, *Weak Decays Beyond Leading Logarithms*, *Rev. Mod. Phys.* to appear [hep-ph/9512380].